A POSTERIORI ERROR ESTIMATORS FOR NON-SYMMETRIC EIGENVALUE PROBLEMS*

JOSCHA GEDICKE AND CARSTEN CARSTENSEN

Abstract. A posteriori error estimators for non-symmetric eigenvalue model problems are discussed in [Heuveline and Rannacher, A posteriori error control for finite element approximations of elliptic eigenvalue problems, 2001] in the context of the dual-weighted residual method (DWR). This paper directly analyses the variational formulation rather than the non-linear ansatz of Becker and Rannacher for some convection-diffusion model problem and presents error estimators for the eigenvalue error based on averaging techniques. In the case of linear P_1 finite elements and globally constant coefficients, the error estimates of the residual and averaging error estimators are refined. Moreover, several postprocessing techniques attached to the DWR paradigm plus two new dual-weighted error estimators are compared in numerical experiments. The first new estimator utilises an auxiliary Raviart-Thomas mixed finite element method and the second exploits an averaging technique in combination with ideas of DWR.

August 7, 2009

1. Introduction

The convection-diffusion model problem for a non-symmetric, elliptic eigenvalue problem reads: Seek an eigenpair $(\lambda, u) \in \mathbb{C} \times H^1_0(\Omega;\mathbb{C}) \cap H^2_{loc}(\Omega;\mathbb{C})$ with

$$-\Delta u + \beta \cdot \nabla u = \lambda u \quad \text{in } \Omega \qquad \text{and} \qquad u = 0 \quad \text{on } \partial\Omega.$$

Suppose that $\beta \in H(div;\mathbb{R}^2)$ is divergence free, $\int_\Omega v \operatorname{div}(\beta)\, dx = 0$ for all $v \in V := H^1_0(\Omega;\mathbb{C})$ on the bounded Lipschitz domain $\Omega \subseteq \mathbb{R}^2$.

The weak problem considers the two complex Hilbert spaces $V := H^1_0(\Omega;\mathbb{C})$ with seminorm $|\!|\!|.|\!|\!| = |.|_{H^1(\Omega;\mathbb{C})}$, which is a norm on V, and $H := L^2(\Omega;\mathbb{C})$ with norm $\|.\|_{L^2(\Omega;\mathbb{C})}$. Seek an eigenpair $(\lambda, u) \in \mathbb{C} \times V$ with $\|u\| = 1$ such that

$$a(u,v) = \lambda b(u,v) \quad \text{for all } v \in V.$$

1991 *Mathematics Subject Classification.* 65N15,65N25,65N30.

Key words and phrases. non-symmetric, eigenvalue, adaptive, finite element method, dual-weighted, DWR.

*Supported by the DFG Research Center MATHEON "Mathematics for key technologies", the WCU program through KOSEF (R31-2008-000-10049-0), and the graduate school BMS "Berlin Mathematical School" in Berlin.

The bilinear form $a(.,.)$ is elliptic and continuous in V and the bilinear form $b(.,.)$ is continuous, symmetric and positive definite, and hence induces a norm $\|.\| := b(.,.)^{1/2}$ on H. For the above model problem, $\|.\| = \|.\|_{L^2(\Omega;\mathbb{C})}$ and the bilinear forms (where $\overline{(.)}$ denotes complex conjugation) are given by

$$a(u,v) = \int_\Omega (\nabla u \cdot \nabla \overline{v} + (\beta \cdot \nabla u)\overline{v})\, dx \qquad \text{and} \qquad b(u,v) = \int_\Omega u\overline{v}\, dx.$$

Since β is assumed to be divergence free, an integration by parts yields

$$\int_\Omega (\beta \cdot \nabla v)\overline{v}\, dx = -\int_\Omega (\beta \cdot \nabla \overline{v}) v\, dx.$$

Hence, for all $v \in V$, it holds

$$|\!|\!| v |\!|\!|^2 = \operatorname{Re} a(v,v).$$

Thus, the ellipticity constant (which is one) of the bilinear form $a(.,.)$ is independent of β.

The analysis of the non-symmetric eigenvalue problem requires the dual eigenvalue problem: Seek a (dual) eigenpair $(\lambda^*, u^*) \in \mathbb{C} \times V$ with $\|u^*\| = 1$ such that

$$a(v,u^*) = \overline{\lambda^*} b(v,u^*) \quad \text{for all } v \in V.$$

Since the embedding of V in H is continuous and compact,

$$V \overset{c}{\hookrightarrow} H,$$

the spectral theory for compact operators [Kat80, OB91] is applicable. The Riesz-Schauder Theorem shows that the primal and dual spectra consist of countable finite or infinite many eigenvalues with no finite accumulation point. In particular the algebraic multiplicities are finite. In the following, suppose that all eigenvalues are simple in the sense that their algebraic multiplicity and hence their geometric multiplicity is one.

The primal λ_j and dual λ_j^* eigenvalues are connected by

$$\lambda_j = \overline{\lambda_j^*} \qquad \text{for } j = 1,2,3,\ldots$$

The dual bilinear form $a^*(u^*,.) := a(.,u^*)$ reads in the model problem

$$a^*(u^*,v) = a(v,u^*) = \int_\Omega (\nabla v \cdot \nabla \overline{u^*} + (\beta \cdot \nabla v)\overline{u^*})\, dx.$$

An integration by parts leads to

$$a^*(u^*,v) = \int_\Omega (\nabla \overline{u^*} \cdot \nabla v - (\beta \cdot \nabla \overline{u^*}) v)\, dx \quad \text{for all } v \in V.$$

Given any finite-dimensional subspace $V_\ell \subset V$, the discrete problems reads: Seek primal and dual (discrete) eigenpairs (λ_ℓ, u_ℓ) and $(\lambda_\ell^*, u_\ell^*)$ with $\|u_\ell\| = 1 = \|u_\ell^*\|$ such that

$$a(u_\ell, v_\ell) = \lambda_\ell b(u_\ell, v_\ell) \quad \text{for all } v_\ell \in V_\ell;$$
$$a(v_\ell, u_\ell^*) = \overline{\lambda_\ell^*} b(v_\ell, u_\ell^*) \quad \text{for all } v_\ell \in V_\ell.$$

The primal and dual discrete eigenvalues are connected by

$$\lambda_{\ell,j} = \overline{\lambda_{\ell,j}^*} \quad \text{for all } j = 1, \dots, \dim(V_\ell).$$

Suppose $\mathcal{T}_\ell$ is a regular triangulation in $\mathbb{R}^2$, e.g., each $T \in \mathcal{T}_\ell$ is a closed triangle, $\overline{\Omega} = \bigcup_{T\in\mathcal{T}_\ell} T$, for any two distinct triangles $T_1, T_2 \in \mathcal{T}_\ell$, $T_1 \cap \mathcal{T}_2$ is either empty or a common vertex or a common side and the minimal angle of every triangle is uniformly bounded from below. The conforming finite element space of order $k \in \mathbb{N}$ for the triangulation $\mathcal{T}_\ell$ is defined by

$$\mathcal{P}_k(\mathcal{T}_\ell) := \big\{ v \in H^1(\Omega;\mathbb{C}) : \forall T \in \mathcal{T}_\ell,\ v_T \text{ is polynomial of degree} \le k \big\}$$

Throughout this paper, let $V_\ell := \mathcal{P}_1(\mathcal{T}_\ell) \cap V$ and $h_\ell \in \mathcal{P}_0(\mathcal{T}_\ell)$ such that $h_{\ell|T} := \operatorname{diam}(T)$ for all $T \in \mathcal{T}_\ell$. Moreover, $a \lesssim b$ denotes an estimate $a \le Cb$ with some generic constant $C > 0$, which is independent of the mesh-size $\|h_\ell\|_{L^\infty(\Omega)}$.

The abstract a priori theory yields the following upper bounds in terms of the maximal mesh-size $\|h_\ell\|_{L^\infty(\Omega)}$,

$$|\lambda - \lambda_\ell| \lesssim \|h_\ell\|_{L^\infty(\Omega)}^{s_1+s_2},$$
$$|||u - u_\ell||| \lesssim \|h_\ell\|_{L^\infty(\Omega)}^{s_1},$$
$$|||u^* - u_\ell^*||| \lesssim \|h_\ell\|_{L^\infty(\Omega)}^{s_2},$$

where $0 < s_1 \le 1$ and $0 < s_2 \le 1$ depend on the regularity of the primal and dual eigenfunctions [OB91, Chapter 10.3].

A posteriori error estimators for symmetric eigenvalue problems (included for $\beta \equiv 0$) can be found in [Ver96, Lar00, DPR03, MSZ06]. The convergence of the adaptive finite element method (AFEM) for the symmetric case is considered in [Sau07, CG08, GMZ08, GG09]. The only known paper on the non-symmetric eigenvalue problem seems to be [HR01]. It is the aim of this paper to review the results of Heuveline and Rannacher in direct approach rather than in the non-linear setting of the DWR paradigm after [BR98, HR01, BR03]. These results are also applicable to the averaging techniques as for the symmetric eigenvalue problem in [MSZ06]. At least for a global constant convection coefficient and linear finite elements on triangles, those estimators are refined as in [CG08].

The numerical experiments indicate that the efficiency indices for the residual-type error estimators depend strongly on the convection coefficient β. Therefore for convection-dominated eigenvalue problems, dual-weighted error estimators are employed. This work compares two

different ways of calculating the dual-weighted residual (DWR) error estimators from [BR98, HR01, BR03] together with two new dual-weighted error estimators. The first new estimator is based on the Raviart-Thomas mixed finite element method (MFEM) of first-order and the second one on averaging techniques and some calculation of the weights. Hence they are named by dual-weighted mixed (DWM) and dual-weighted averaging (DWA) estimator.

The outline of the remaining parts of this paper is a follows. In Section 2 an optimal error estimate for the eigenvalue error is derived. Therefore, the basic algebraic properties and identities of the non-symmetric eigenvalue problem are revised. In contrast to [HR01], the direct variational formulation is used, rather then the more general non-linear framework of Becker and Rannacher [BR98, BR03] in the DWR paradigm. The weak regularity assumptions and the suboptimal L^2 error estimate of [HR01] prove the L^2 contribution to the residual identity of higher-order. Section 3 summarises some old and some new results on several a posteriori error estimators, namely the residual, the averaging, the reduced residual and averaging estimators. The dual-weighted error estimators, namely the two DWR, the DWM and the DWA error estimators, are presented in Section 4. Section 5 compares the error estimators in numerical benchmarks on three different domains and with various convection coefficients.

This paper employs standard notation on Lebesgue and Sobolev spaces and norms.

2. Algebraic properties

This section concerns the primal and dual residual and the estimation of the eigenvalue error and the energy error in the primal and dual eigenfunctions.

For the primal and dual discrete eigenpairs (λ_ℓ, u_ℓ) and $(\lambda_\ell^*, u_\ell^*)$, the residuals are defined

$$\begin{aligned}\mathrm{Res}_\ell &:= a(u_\ell, \cdot) - \lambda_\ell b(u_\ell, \cdot) \in V^*;\\ \mathrm{Res}_\ell^* &:= a(\cdot, u_\ell^*) - \overline{\lambda}_\ell^* b(\cdot, u_\ell^*) \in V^*.\end{aligned}$$

It is the goal of this section to derive the following optimal error estimate for the eigenvalues

$$|\lambda - \lambda_\ell| \lesssim |\!|\!| \mathrm{Res}_\ell |\!|\!|_*^2 + |\!|\!| \mathrm{Res}_\ell^* |\!|\!|_*^2. \tag{2.1}$$

The authors of this paper expect that this estimate was known to the authors of [HR01] as well. They speculated that the main critics on this estimate is the lack of locality aimed at DWR. However, the authors believe that (2.1) is sharp. The starting point of the analysis of (2.1) is a connection between the eigenvalue error and the primal and dual residuals. The combination of a suboptimal L^2 error estimate from [HR01] with a suboptimal error estimate for the eigenvalue error leads

to an optimal error estimate for the energy error. An application of this estimate to the primal-dual error residual identity, stated below, will then yield the optimal estimate for the eigenvalue error.

Lemma 2.1 (Primal-Dual Error Residual Identity)**.** *Suppose* (λ_ℓ, u_ℓ) *is an approximation to the primal eigenpair* (λ, u) *and* $(\lambda_\ell^*, u_\ell^*)$ *is an approximation to the corresponding dual eigenpair* (λ^*, u^*) *and set* $e_\ell := u - u_\ell$ *and* $e_\ell^* := u^* - u_\ell^*$*. Then it holds*

$$(\lambda - \lambda_\ell)\big(b(u, u^*) + b(u_\ell, u_\ell^*) - b(e_\ell, e_\ell^*)\big) = Res_\ell(e_\ell^*) + Res_\ell^*(e_\ell).$$

Proof. Direct algebraic manipulations and the definition of the residuals plus $\lambda = \overline{\lambda^*}$, $\lambda_\ell = \overline{\lambda_\ell^*}$ lead to

$$\begin{aligned} a(u_\ell, u^* - u_\ell^*) - \lambda_\ell b(u_\ell, u^* - u_\ell^*) + a(u - u_\ell, u_\ell^*) - \overline{\lambda_\ell^*} b(u - u_\ell, u_\ell^*) \\ &= a(u_\ell, u^*) - \lambda_\ell b(u_\ell, u^*) + a(u, u_\ell^*) - \overline{\lambda_\ell^*} b(u, u_\ell^*) \\ &= (\overline{\lambda^*} - \lambda_\ell) b(u_\ell, u^*) + (\lambda - \overline{\lambda_\ell^*}) b(u, u_\ell^*) \\ &= (\lambda - \lambda_\ell)(b(u, u^*) + b(u_\ell, u_\ell^*) - b(e_\ell, e_\ell^*)). \end{aligned}$$ □

Lemma 2.2. *Suppose that the maximal mesh-size* $\|h_\ell\|_{L^\infty(\Omega)}$ *tends to zero as* $\ell \to \infty$*, then*

$$\lim_{\ell\to\infty} b(e_\ell, e_\ell^*) = 0 \qquad \textit{and} \qquad \lim_{\ell\to\infty} b(u_\ell, u_\ell^*) = b(u, u^*).$$

Proof. The convergence of $|||e_\ell|||$ and $|||e_\ell^*|||$ implies the convergence of $\|e_\ell\|$ and $\|e_\ell^*\|$ to zero as $\ell \to \infty$ because of the compact embedding. Hence the assertions follow from $|b(e_\ell, e_\ell^*)| \le \|e_\ell\|\|e_\ell^*\|$ and

$$|b(u, u^*) - b(u_\ell, u_\ell^*)| = |b(u - u_\ell, u^*) + b(u_\ell, u^* - u_\ell^*)| \le \|e_\ell\|\|e_\ell^*\|. \square$$

Remark 2.1. Since all eigenvalues converge as $\|h_\ell\|_{L^\infty(\Omega)} \to 0$, λ_ℓ is, as λ, a simple eigenvalue for sufficiently small $\|h_\ell\|_{L^\infty(\Omega)}$. The condition number $1/|y_\ell^H x_\ell|$ of the discrete eigenvalue λ_ℓ is defined for right and left eigenvectors x_ℓ and y_ℓ of the algebraic eigenvalue problems

$$A_\ell x_\ell = \lambda_\ell x_\ell \quad \text{and} \quad y_\ell^H A_\ell = \overline{\lambda_\ell^*} y_\ell^H.$$

It is shown in [GV96] that $y_\ell^H x_\ell \neq 0$ for simple eigenvalues. Therefore it holds $b(u_\ell, u_\ell^*) \neq 0$. In addition $|y_\ell^H x_\ell| \ll 1$ implies that A_ℓ is close to a matrix with a multiple eigenvalue λ_ℓ. Hence it is reasonable to assume $b(u, u^*) \neq 0$. Furthermore, $1/|b(u, u^*)|$ is the condition of the continuous eigenvalue λ and

$$|b(u, u^*) + b(u_\ell, u_\ell^*) - b(e_\ell, e_\ell^*)| \longrightarrow 2|b(u, u^*)|$$

as $\|h_\ell\|_{L^\infty(\Omega)} \to 0$.

Suppose $b(u, u^*) \neq 0$ and let the maximal mesh-size $\|h_\ell\|_{L^\infty(\Omega)}$ of the triangulation $\mathcal{T}_\ell$ be sufficiently small, i.e.

$$\begin{aligned} \max\{|||e_\ell|||, |||e_\ell^*|||, \|e_\ell\|, \|e_\ell^*\|, |\lambda - \lambda_\ell|, 2|b(u, u^*) - b(u_\ell, u_\ell^*)|\} \\ < \min\{1, |b(u, u^*)|\}, \end{aligned} \tag{2.2}$$

then $|b(u,u^*)|/2 < |b(u,u^*) + b(u_\ell,u_\ell^*) - b(e_\ell,e_\ell^*)| < 3$ and it holds

$$|\lambda - \lambda_\ell| \approx |\mathrm{Res}_\ell(e_\ell^*) + \mathrm{Res}_\ell^*(e_\ell)|.$$

This implies the suboptimal eigenvalue error estimate

$$|\lambda - \lambda_\ell| \lesssim |\!|\!|\mathrm{Res}_\ell|\!|\!|_* + |\!|\!|\mathrm{Res}_\ell^*|\!|\!|_*. \tag{2.3}$$

In addition, the suboptimal L^2 error estimates

$$\|e_\ell\| \lesssim |\!|\!|\mathrm{Res}_\ell|\!|\!|_* + |\lambda - \lambda_\ell| \quad \text{and} \quad \|e_\ell^*\| \lesssim |\!|\!|\mathrm{Res}_\ell^*|\!|\!|_* + |\lambda - \lambda_\ell| \tag{2.4}$$

from Heuveline and Rannacher [HR01, (70)-(71)] are used in the proof of the following lemma.

Remark 2.2. The proof of the suboptimal L^2 error estimate in [HR01] is based on the weak regularity assumption of the eigenvalue λ with the eigenspace $E(\lambda)$, that $a_\lambda(.,.) = a(.,.) - \lambda b(.,.)$ is regular on the quotient space $V/E(\lambda)$, namely

$$|\!|\!|w|\!|\!| \le C_\lambda \sup_{v \in V/E(\lambda)} \frac{a_\lambda(v,w)}{|\!|\!|v|\!|\!|} \quad \text{for all } w \in V/E(\lambda).$$

The weak stability constant C_λ depends on the distance of λ to all other distinct eigenvalues and does not depend on the mesh-size.

Lemma 2.3 (Energy Estimate)**.** *Suppose $b(u,u^*) \neq 0$, the maximal mesh-size $\|h_\ell\|_{L^\infty(\Omega)}$ is sufficiently small according to* (2.2) *and (λ_ℓ, u_ℓ) is an approximation to the primal eigenpair (λ, u) and $(\lambda_\ell^*, u_\ell^*)$ is an approximation to the corresponding dual eigenpair (λ^*, u^*) and set $e_\ell := u - u_\ell$ as well as $e_\ell^* := u^* - u_\ell^*$. Then it holds*

$$|\!|\!|e_\ell|\!|\!| + |\!|\!|e_\ell^*|\!|\!| \lesssim |\!|\!|Res_\ell|\!|\!|_* + |\!|\!|Res_\ell^*|\!|\!|_*.$$

Proof. Observe that

$$\begin{aligned} a(e_\ell,e_\ell) &= \lambda + \lambda_\ell - \lambda b(u,u_\ell) - a(u_\ell,u) \\ &= (\lambda+\lambda_\ell)(1 - \mathrm{Re}\, b(u,u_\ell)) + i\,(\lambda_\ell - \lambda)\mathrm{Im}\, b(u,u_\ell) \\ &\quad + \lambda_\ell b(u_\ell,u) - a(u_\ell,u) \\ &= (\lambda+\lambda_\ell)(1 - \mathrm{Re}\, b(u,u_\ell)) + i\,(\lambda_\ell - \lambda)\mathrm{Im}\, b(u-u_\ell,u_\ell) \\ &\quad + \lambda_\ell b(u_\ell,u) - a(u_\ell,u). \end{aligned}$$

The last inequality follows from $0 = \mathrm{Im}\|u_\ell\|^2$. Since

$$2\mathrm{Re}\, b(u,u_\ell) = \|u\|^2 + \|u_\ell\|^2 - \|e_\ell\|^2 = 2 - \|e_\ell\|^2,$$

this implies

$$|\!|\!|e_\ell|\!|\!|^2 = \mathrm{Re}\, a(e_\ell,e_\ell) \le |\mathrm{Res}_\ell(e_\ell)| + |\lambda - \lambda_\ell|\|e_\ell\| + \frac{|\lambda+\lambda_\ell|}{2}\|e_\ell\|^2.$$

The suboptimal estimates (2.3) and (2.4) imply

$$|\lambda - \lambda_\ell| + \|e_\ell\| \lesssim |\!|\!|\mathrm{Res}_\ell|\!|\!|_* + |\!|\!|\mathrm{Res}_\ell^*|\!|\!|_*.$$

Since $\|.\| \lesssim |||.|||$, the aforementioned inequalities yield

$$|||e_\ell||| \lesssim |||\mathrm{Res}_\ell|||_* + |||\mathrm{Res}^*_\ell|||_*.$$

Similarly it follows

$$|||e^*_\ell||| \lesssim |||\mathrm{Res}_\ell|||_* + |||\mathrm{Res}^*_\ell|||_*. \qquad \square$$

Theorem 2.4 (Eigenvalue Error Estimate)**.** *Suppose $b(u, u^*) \neq 0$, the maximal mesh-size $\|h_\ell\|_{L^\infty(\Omega)}$ is sufficiently small such that (2.2) holds and let (λ_ℓ, u_ℓ) be an approximation to (λ, u) and $(\lambda^*_\ell, u^*_\ell)$ an approximation to the corresponding dual eigenpair (λ^*, u^*), then it holds*

$$|\lambda - \lambda_\ell| \lesssim |||Res_\ell|||^2_* + |||Res^*_\ell|||^2_*.$$

Proof. The aforementioned Lemma 2.3 and the Cauchy-Schwarz inequality lead to

$$|\lambda - \lambda_\ell| \lesssim |\mathrm{Res}_\ell(e^*_\ell)| + |\mathrm{Res}^*_\ell(e_\ell)| \lesssim |||\mathrm{Res}_\ell|||^2_* + |||\mathrm{Res}^*_\ell|||^2_*. \qquad \square$$

3. A Posteriori Error Estimates

This section is devoted to the residual error estimator from [HR01], the averaging technique of [Car03], plus a refinement (similar as in [CG08]) for globally constant coefficients. These error estimators involve constants, which depend strongly on the size of the convection coefficient. Throughout this section it is assumed that the conditions of Theorem 2.4 are satisfied and that (λ_ℓ, u_ℓ) is an approximation to the primal eigenpair (λ, u) and $(\lambda^*_\ell, u^*_\ell)$ is an approximation to the dual eigenpair (λ^*, u^*).

Given a regular triangulation $\mathcal{T}_\ell$, define $\mathcal{E}_\ell$ as the set of inner edges and $\mathcal{N}_\ell$ as the set of inner nodes. Let $h_T := \mathrm{diam}(T)$ for $T \in \mathcal{T}_\ell$ and $h_E := \mathrm{diam}(E)$ for $E \in \mathcal{E}_\ell$. For a $\mathcal{P}_1$ finite element solution $u_\ell \in V_\ell$ on the triangulation $\mathcal{T}_\ell$ let $p_\ell := \nabla u_\ell$ denote the discrete piecewise constant gradient. It's jump in normal direction ν_E along an inner edge $\partial T_+ \cap \partial T_- = E \in \mathcal{E}_\ell$, for $T_+, T_- \in \mathcal{T}_\ell$, is denoted by

$$[p_\ell]\cdot\nu_E = p_\ell|_{T_+}\cdot\nu_E - p_\ell|_{T_-}\cdot\nu_E.$$

Lemma 3.1. *It holds*

$$|||Res_\ell|||^2_* \lesssim \eta^2_\ell := \sum_{T\in\mathcal{T}_\ell} h^2_T \|\beta\cdot p_\ell - \lambda_\ell u_\ell\|^2_{L^2(T)} + \sum_{E\subset T} h_E \|[p_\ell]\cdot\nu_E\|^2_{L^2(E)},$$

$$|||Res^*_\ell|||^2_* \lesssim \eta^{*^2}_\ell := \sum_{T\in\mathcal{T}_\ell} h^2_T \|-\beta\cdot\overline{p^*_\ell} - \overline{\lambda^*_\ell u^*_\ell}\|^2_{L^2(T)} + \sum_{E\subset T} h_E \|[\overline{p^*_\ell}]\cdot\nu_E\|^2_{L^2(E)}.$$

Proof. Let v_ℓ denote the Scott-Zhang interpolation of v onto V_ℓ, then it holds

$$\begin{aligned}\mathrm{Res}_\ell(v) &= \mathrm{Res}_\ell(v - v_\ell) = a(u_\ell, v - v_\ell) - \lambda_\ell b(u_\ell, v - v_\ell)\\ &= \sum_{T\in\mathcal{T}_\ell}\int_T p_\ell\cdot\nabla(\overline{v - v_\ell}) + \beta\cdot p_\ell(\overline{v - v_\ell})dx - \lambda_\ell\int_T u_\ell(\overline{v - v_\ell})dx\\ &= \sum_{T\in\mathcal{T}_\ell}\int_T(\beta\cdot p_\ell - \lambda_\ell u_\ell)(\overline{v - v_\ell})dx + \sum_{E\in\mathcal{E}_\ell}\int_E [p_\ell]\cdot\nu_E(\overline{v - v_\ell})ds.\end{aligned}$$

The approximation property of the interpolation operator

$$\sum_{T\in\mathcal{T}_\ell}\|h_T^{-1}(v - v_\ell)\|^2_{L^2(T)} + \sum_{E\in\mathcal{E}_\ell}\|h_E^{-1/2}(v - v_\ell)\|^2_{L^2(E)} \lesssim |\!|\!| v |\!|\!|^2$$

and the Cauchy-Schwarz inequality yield

$$\begin{aligned}\mathrm{Res}_\ell(v) &\le \sum_{T\in\mathcal{T}} h_T\|\beta\cdot p_\ell - \lambda_\ell u_\ell\|_{L^2(T)}\|h_T^{-1}(v - v_\ell)\|_{L^2(T)}\\ &\quad + \sum_{E\in\mathcal{E}} h_E^{1/2}\|[p_\ell]\cdot\nu_E\|_{L^2(E)}\|h_E^{-1/2}(v - v_\ell)\|_{L^2(E)}\\ &\lesssim \eta_\ell |\!|\!| v |\!|\!|.\end{aligned}$$

The same arguments lead to the assertion for $|\!|\!|\mathrm{Res}^*_\ell|\!|\!|$. □

The averaging technique concerns averaging operators $A : V_\ell^d \to \mathcal{S}^1(\mathcal{T}_\ell)^d := V_\ell^d \cap \mathcal{C}(\Omega)^d$ with the model example

$$A(p_\ell) := \sum_{z\in\mathcal{N}_\ell}\frac{1}{|\omega_z|}\left(\int_{\omega_z} p_\ell\,dx\right)\varphi_z.$$

Here and throughout this paper, φ_z denotes the nodal basis function for an inner node $z \in \mathcal{N}_\ell$. Alternative averaging operators from [Car03] could be employed as well.

Lemma 3.2. *For*

$$\begin{aligned}\mu_\ell &:= \|h_\ell(-div(A(p_\ell)) + \beta\cdot p_\ell - \lambda_\ell u_\ell)\|_{L^2(\Omega)} + \|A(p_\ell) - p_\ell\|_{L^2(\Omega)},\\ \mu^*_\ell &:= \|h_\ell(-div(A(\overline{p^*_\ell})) - \beta\cdot\overline{p^*_\ell} - \overline{\lambda^*_\ell u^*_\ell})\|_{L^2(\Omega)} + \|A(\overline{p^*_\ell}) - \overline{p^*_\ell}\|_{L^2(\Omega)}\end{aligned}$$

it holds

$$|\!|\!| Res_\ell |\!|\!|_* \lesssim \mu_\ell \qquad \text{and} \qquad |\!|\!| Res^*_\ell |\!|\!|_* \lesssim \mu^*_\ell.$$

Proof. As in the previous lemma, let v_ℓ denote the Scott-Zhang interpolation of v onto V_ℓ, since $A(p_\ell)$ is globally continuous the divergence

theorem can be applied. This yields

$$\begin{aligned}\mathrm{Res}_\ell(v) &= \mathrm{Res}_\ell(v - v_\ell) = a(u_\ell, v - v_\ell) - \lambda_\ell b(u_\ell, v - v_\ell) \\ &= \int_\Omega (p_\ell - A(p_\ell))\nabla(\overline{v - v_\ell})dx - \int_\Omega \mathrm{div}(A(p_\ell))(\overline{v - v_\ell})dx \\ &\quad + \int_\Omega (\beta \cdot p_\ell - \lambda_\ell u_\ell)(\overline{v - v_\ell})dx.\end{aligned}$$

Hölder's inequality leads to

$$\begin{aligned}\mathrm{Res}_\ell(v) \leq \sum_{T\in\mathcal{T}_\ell} h_T \|-\mathrm{div}(A(p_\ell)) + \beta\cdot p_\ell - \lambda_\ell u_\ell\|_{L^2(T)} \|h_T^{-1}(v - v_\ell)\|_{L^2(T)} \\ + \sum_{T\in\mathcal{T}_\ell} \|p_\ell - A(p_\ell)\|_{L^2(T)} \|\nabla(v - v_\ell)\|_{L^2(T)}.\end{aligned}$$

Using the stability and the afore mentioned approximation property

$$\sum_{T\in\mathcal{T}_\ell} \|\nabla v_\ell\|^2_{L^2(T)} \lesssim |\!|\!| v |\!|\!|^2 \quad \text{and} \quad \sum_{T\in\mathcal{T}_\ell} \|h_T^{-1}(v - v_\ell)\|^2_{L^2(T)} \lesssim |\!|\!| v |\!|\!|^2,$$

together with the Cauchy-Schwarz inequality yield

$$\mathrm{Res}_\ell(v) \lesssim \mu_\ell |\!|\!| v |\!|\!|.$$

In the same way the assertion $|\!|\!|\mathrm{Res}^*_\ell|\!|\!| \lesssim \mu^*$ is satisfied. □

Similar to the case of symmetric eigenvalue problems accordingly to [CG08] these two error estimators can be improved by using the H^1 stability of the L^2 projection [Car04]. The stability and approximation properties are proven for triangular elements under the assumptions that $d = 2$ and that the triangulation is refined using the red-green-blue algorithm. The enhancing is only possible assuming a globally constant convection coefficient β.

Lemma 3.3. *Suppose that the convection coefficient β is globally constant, then for linear $\mathcal{P}_1$-FE on triangles (d=2) it holds*

$$\begin{aligned}|\!|\!| Res_\ell |\!|\!|^2_* &\lesssim \eta^2_{\ell,reduced} := \sum_{E\in\mathcal{E}_\ell} h_E \big\| [p_\ell]\cdot\nu_E \big\|^2_{L^2(E)}, \\ |\!|\!| Res^*_\ell |\!|\!|^2_* &\lesssim \eta^{*2}_{\ell,reduced} := \sum_{E\in\mathcal{E}_\ell} h_E \big\| [\overline{p^*_\ell}]\cdot\nu_E \big\|^2_{L^2(E)}.\end{aligned}$$

Proof. Let v_ℓ be the L^2 projection of v in V_ℓ which is H^1 stable by the assumptions. Then it holds

$$\begin{aligned}\mathrm{Res}_\ell(v) &= \mathrm{Res}_\ell(v - v_\ell) = a(u_\ell, v - v_\ell) - \lambda_\ell b(u_\ell, v - v_\ell) = a(u_\ell, v - v_\ell)\\ &= \int_\Omega p_\ell \cdot \nabla(\overline{v - v_\ell})dx + \int_\Omega (\beta \cdot p_\ell)(\overline{v - v_\ell})dx\\ &= \int_\Omega p_\ell \cdot \nabla(\overline{v - v_\ell})dx + \int_\Omega (\beta \cdot p_\ell - \beta \cdot A(p_\ell))(\overline{v - v_\ell})dx\\ &= \sum_{E\in\mathcal{E}_\ell} \int_E [p_\ell] \cdot \nu_E(\overline{v - v_\ell})\, ds + \sum_{T\in\mathcal{T}_\ell} \int_T (\beta \cdot p_\ell - \beta \cdot A(p_\ell))(\overline{v - v_\ell})dx.\end{aligned}$$

Hölder's inequality and the approximation property of the L^2 projection

$$\sum_{T\in\mathcal{T}_\ell} \|h_T^{-1}(v - v_\ell)\|^2_{L^2(T)} + \sum_{E\in\mathcal{E}_\ell} \|h_E^{-1/2}(v - v_\ell)\|^2_{L^2(E)} \lesssim |\!|\!| v |\!|\!|^2.$$

lead to

$$\mathrm{Res}_\ell(v) \lesssim \eta_\ell |\!|\!| v |\!|\!| + \|\beta\|_{L^\infty(\Omega;\mathbb{C})} \left(\sum_{T\in\mathcal{T}_\ell} h_T^2 \|p_\ell - A(p_\ell)\|^2_{L^2(\Omega)} \right)^{1/2} |\!|\!| v |\!|\!|.$$

Because of the well known fact that the averaging estimator is equivalent to the edge-residual estimator [Ver96], it holds

$$|\!|\!| \mathrm{Res}_\ell |\!|\!| \lesssim (1 + \|h_\ell\|_{L^\infty(\Omega)} \|\beta\|_{L^\infty(\Omega;\mathbb{C})}) \eta_\ell.$$

Using the same argumentation results in

$$|\!|\!| \mathrm{Res}^*_\ell |\!|\!|_* \lesssim (1 + \|h_\ell\|_{L^\infty(\Omega)} \|\beta\|_{L^\infty(\Omega;\mathbb{C})}) \eta^*_\ell. \qquad \square$$

Again assuming a globally constant convection coefficient β, the averaging error estimator can be improved for linear finite elements, by showing that a second volumetric part is not needed. This will be proven using the H^1 stability of the L^2 projection.

Lemma 3.4. *Suppose that the convection coefficient β is globally constant, then for linear $\mathcal{P}_1$-FE on triangles (d=2) it holds*

$$\begin{aligned}|\!|\!| Res_\ell |\!|\!|_* &\lesssim \mu_{\ell,reduced} := \|A(p_\ell) - p_\ell\|_{L^2(\Omega)},\\ |\!|\!| Res^*_\ell |\!|\!|_* &\lesssim \mu_{\ell,reduced} := \|A(\overline{p^*_\ell}) - \overline{p^*_\ell}\|_{L^2(\Omega)}.\end{aligned}$$

Proof. Let v_ℓ be the L^2 projection of v in V_ℓ which is H^1 stable by the assumptions. Since $A(p_\ell)$ is globally continuous, the divergence theorem is globally applicable. Notice that for the finite dimensional subspace V_ℓ there holds the local discrete inverse inequality

$$\|h_T \mathrm{div}(v_\ell)\|_{L^2(T)} \le C_{inv} \|v_\ell\|_{L^2(T)}.$$

Together with the approximation property

$$\sum_{T\in\mathcal{T}_\ell} \|h_T^{-1}(v - v_\ell)\|^2_{L^2(T)} \lesssim |\!|\!| v |\!|\!|^2$$

it follows

$$\begin{aligned}-\int_\Omega A(p_\ell)\nabla(\overline{v-v_\ell})\,dx &= \int_\Omega (\overline{v-v_\ell})\mathrm{div}(A(p_\ell))\,dx\\ &= \sum_T \int_T h_T \mathrm{div}(A(p_\ell))h_T^{-1}(\overline{v-v_\ell})\,dx\\ &\le C_{inv}\sum_T \|A(p_\ell)-p_\ell\|_{L^2(T)}\|h_T^{-1}(v-v_\ell)\|_{L^2(T)}\\ &\lesssim \|A(p_\ell)-p_\ell\|_{L^2(\Omega)}|\!|\!|v|\!|\!|.\end{aligned}$$

From this and the stability of the L^2 projection

$$\sum_{T\in\mathcal{T}_\ell}\|\nabla v_\ell\|^2_{L^2(T)} \lesssim |\!|\!|v|\!|\!|^2,$$

it is concluded

$$\begin{aligned}\mathrm{Res}_\ell(v) = \mathrm{Res}_\ell(v-v_\ell) &= a(u_\ell, v-v_\ell) - \lambda_\ell b(u_\ell, v-v_\ell) = a(u_\ell, v-v_\ell)\\ &= \int_\Omega (p_\ell - A(p_\ell))\nabla(\overline{v-v_\ell})dx + \int_\Omega A(p_\ell)\nabla(\overline{v-v_\ell})dx\\ &\qquad + \int_\Omega (\beta\cdot p_\ell - \beta\cdot A(p_\ell))(\overline{v-v_\ell})dx\\ &\lesssim (1+\|h_\ell\|_{L^\infty(\Omega)}\|\beta\|_{L^\infty(\Omega;\mathbb{C})})\mu_\ell |\!|\!|v|\!|\!|.\end{aligned}$$

Using the same argumentation results in

$$|\!|\!|\mathrm{Res}^*_\ell|\!|\!|_* \lesssim (1+\|h_\ell\|_{L^\infty(\Omega)}\|\beta\|_{L^\infty(\Omega;\mathbb{C})})\mu^*_\ell. \qquad \square$$

4. Dual-Weighted a Posteriori Error Estimates

After four different residual or averaging based error estimators have been derived, dual-weighted error estimators will be concerned. The main drawback of the residual or averaging error estimators is that their proofs use stability and approximation properties which involve constants that depend strongly on the size of the convection coefficient β. The dual-weighted error estimators in general avoid any inequality with unknown constants. Thus they are robust with respect to strong convection which is also confirmed by the numerical examples in Section 5.

Throughout this section it is assumed that $b(u,u^*)\neq 0$, the maximal mesh-size $\|h_\ell\|_{L^\infty(\Omega)}$ is sufficiently small such that (2.2) holds, (λ_ℓ, u_ℓ) is an approximation to the primal eigenpair (λ, u), $(\lambda^*_\ell, u^*_\ell)$ is an approximation to the corresponding dual eigenpair (λ^*, u^*), $e_\ell := u - u_\ell$ and $e^*_\ell := u^* - u^*_\ell$.

The dual-weighted error estimators are based on the inequality

$$|\lambda - \lambda_\ell| \lesssim |\mathrm{Res}_\ell(e^*_\ell) + \mathrm{Res}^*_\ell(e_\ell)|,$$

which follows directly from Lemma 2.1 and Lemma 2.2 for sufficiently small mesh sizes. Observe that the constant in this inequality tends

to $1/(2|b(u,u^*)|)$ as $\|h_\ell\|_{L^\infty(\Omega)} \to 0$. One question that arises from the computation of $\mathrm{Res}_\ell(e_\ell^*)$ or $\mathrm{Res}_\ell^*(e_\ell)$ is the calculation of the unknown errors e_ℓ and e_ℓ^*. The rather heuristic approach of [BR03] states that it is numerically reliable and efficient to approximate these quantities which occur only in the weights. The idea is that one does not need to approximate the weights with higher accuracy than the size of the residual terms. In practice the unknown primal and dual solutions u, u^* are replaced by solutions of a higher-order method or by higher-order interpolation. In Section 5 a higher-order interpolation ansatz is described which leads to numerically reliable and efficient dual-weighted error estimators.

In the following, four different dual-weighted error estimators are presented. The first one is derived from the classical dual-weighted residual (DWR) ansatz as in [HR01] or [BR03], the second follows a modern approach of dealing with the weights as described in [BR03]. Afterwards a new (DWM) error estimator for the eigenvalue error which utilises a non standard finite element solution of a mixed auxiliary problem in the Raviart-Thomas space of order zero is derived. This is followed by a new (DWA) error estimator in the spirit of [BR03] using the averaging technique instead of residuals.

To begin with, the classical DWR error estimator is stated.

Lemma 4.1. *Let the eigenfunctions $u, u^* \in H^2(\Omega) \cap H^3(\mathcal{T}_\ell)$ and*

$$\begin{aligned} \eta_T &:= \|\beta\cdot p_\ell - \lambda_\ell u_\ell\|_{L^2(T)} + h_T^{-1/2}\|[p_\ell]\cdot\nu_E\|_{L^2(\partial T)}, \\ \eta_T^* &:= \|-\beta\cdot\overline{p_\ell^*} - \overline{\lambda_\ell^* u_\ell^*}\|_{L^2(T)} + h_T^{-1/2}\|[\overline{p_\ell^*}]\cdot\nu_E\|_{L^2(\partial T)}. \end{aligned} \tag{4.1}$$

Then it holds

$$\begin{aligned} |\lambda - \lambda_\ell| \lesssim \eta_{\ell,DWR1} := &\sum_{T\in\mathcal{T}_\ell} h_T^{3/2}\eta_T \left(\|[p_\ell^*]\cdot\nu_E\|_{L^2(\bigcup \mathcal{E}_{\Omega_T})} + h.o.t.\right) \\ &+ \sum_{T\in\mathcal{T}_\ell} h_T^{3/2}\eta_T^* \left(\|[p_\ell]\cdot\nu_E\|_{L^2(\bigcup \mathcal{E}_{\Omega_T}))} + h.o.t.\right) \end{aligned}$$

for higher-order terms (h.o.t.) and suitable fixed subsets $\Omega_T \subseteq \Omega$ which contain $T \in \mathcal{T}_\ell$, and with skeleton $\bigcup \mathcal{E}_{\Omega_T}$.

Proof. Suppose $u \in H^2(\Omega)$, integration by parts and Hölder's inequality show

$$\begin{aligned} \mathrm{Res}_\ell(v) &= \sum_{T\in\mathcal{T}_\ell} \int_T p_\ell\cdot\nabla(\overline{v - v_\ell}) + (\beta\cdot p_\ell - \lambda_\ell u_\ell)(\overline{v - v_\ell})dx \\ &\le \sum_{T\in\mathcal{T}_\ell} h_T^{-1/2}\|[p_\ell]\cdot\nu_E\|_{L^2(\partial T)} h_T^{1/2}\|v - v_\ell\|_{L^2(\partial T)} \\ &\qquad + \|\beta\cdot p_\ell - \lambda_\ell u_\ell\|_{L^2(T)}\|v - v_\ell\|_{L^2(T)} \\ &\le \sum_{T\in\mathcal{T}_\ell} \eta_T\omega_T. \end{aligned}$$

Therein, η_T is defined in (4.1) and

$$\omega_T := \|v - v_\ell\|_{L^2(T)} + h_T^{1/2}\|v - v_\ell\|_{L^2(\partial T)}.$$

Let $v_\ell = \mathcal{I}_\ell v \in V_\ell$ be the nodal interpolant of v. The interpolation estimate

$$\|v - \mathcal{I}_\ell v\|^2_{L^2(T)} + h_T\|v - \mathcal{I}_\ell v\|^2_{L^2(\partial T)} \lesssim h_T^4\|D^2 v\|^2_{L^2(T)}$$

leads to

$$\mathrm{Res}_\ell(v) \lesssim \sum_{T\in\mathcal{T}_\ell} h_T^2\eta_T\|D^2 v\|_{L^2(T)}.$$

In [HR01] $D^2 v$ is locally approximated on each quadrilateral $Q \in \mathcal{Q}_\ell$ by $D^2 v_\ell|_Q$ using finite differences. While this is a appropriate ansatz for quadrilateral meshes, for general triangular meshes this is not suited. In [Car05a] it is shown, $v \in H^3(\mathcal{T}_\ell)$ implies

$$\|D^2 v\|_{L^2(T)} \le c_1 h_T^{-1/2}\|[\nabla v_\ell]\cdot\nu_E\|_{L^2(\bigcup \mathcal{E}_{\Omega_T}))} + c_2\|\nabla(v - v_\ell)\|^{1/2}_{L^2(\Omega_T)}.$$

The constant c_1 depends on the shape of elements and c_2 on $\|v\|_{H^3(\Omega_T)}$. The second term on the right hand side is of higher-order. This leads to the estimate

$$|\mathrm{Res}_\ell(e_\ell^*)| \lesssim \sum_{T\in\mathcal{T}_\ell} h_T^{3/2}\eta_T\left(\|[p_\ell^*]\cdot\nu_E\|_{L^2(\bigcup \mathcal{E}_{\Omega_T})} + \text{h.o.t.}\right).$$

In the same way it is shown that

$$|\mathrm{Res}_\ell^*(e_\ell)| \lesssim \sum_{T\in\mathcal{T}_\ell} h_T^{3/2}\eta_T^*\left(\|[p_\ell]\cdot\nu_E\|_{L^2(\bigcup \mathcal{E}_{\Omega_T})} + \text{h.o.t.}\right). \qquad \square$$

Remark 4.1. From the theory in [Car05a] it remains open to choose the fixed size of the patches Ω_T containing $T \in \mathcal{T}_\ell$. However, the numerical examples of Section 5 suggest, that, surprisingly, $\Omega_T = T$ and thus $\bigcup \mathcal{E}_{\Omega_T} = \partial T$ might be sufficient.

The drawback of this classical approach is that the constant in the interpolation estimate depends on the size of the convection coefficient. Therefore the nowadays common approach is to stop even further in the estimates. The modern dual-weighted residual (DWR) estimate accordingly to [BR03] reads as follows. Observe that these error estimators involve the unknown exact primal and dual errors e_ℓ and e_ℓ^*. In the numerical examples of Section 5, these errors have to be approximated.

Lemma 4.2. *For the unknown exact errors e_ℓ and e_ℓ^* let*

$$\eta := \sum_{T\in\mathcal{T}_\ell}\int_T(\beta\cdot p_\ell - \lambda_\ell u_\ell)\overline{e_\ell^*}dx + \sum_{E\in\mathcal{E}_\ell}\int_E([p_\ell]\cdot\nu_E)\overline{e_\ell^*}ds,$$

$$\eta^* := \sum_{T\in\mathcal{T}_\ell}\int_T(-\beta\cdot\overline{p_\ell^*} - \overline{\lambda_\ell^* u_\ell^*})e_\ell dx + \sum_{E\in\mathcal{E}_\ell}\int_E([\overline{p_\ell^*}]\cdot\nu_E)e_\ell ds.$$

Then it holds

$$|\lambda - \lambda_\ell| \lesssim \eta_{\ell,DWR2} := |\eta + \eta^*|.$$

Proof. Integration by parts leads to

$$\begin{aligned}\mathrm{Res}_\ell(e_\ell^*) &= a(u_\ell, u^* - u_\ell^*) - \lambda_\ell b(u_\ell, u^* - u_\ell^*)\\ &= \sum_{T\in\mathcal{T}_\ell}\int_T (\beta\cdot p_\ell - \lambda_\ell u_\ell)\overline{(u^* - u_\ell^*)}dx + \sum_{E\in\mathcal{E}_\ell}\int_E [p_\ell]\cdot\nu_E\overline{(u^* - u_\ell^*)}ds,\end{aligned}$$

respectively,

$$\begin{aligned}\mathrm{Res}_\ell^*(e_\ell) &= a(u - u_\ell, u_\ell^*) - \overline{\lambda_\ell^*} b(u - u_\ell, u_\ell^*)\\ &= \sum_{T\in\mathcal{T}_\ell}\int_T (-\beta\cdot\overline{p_\ell^*} - \overline{\lambda_\ell^* u_\ell^*})(u - u_\ell)dx + \sum_{E\in\mathcal{E}_\ell}\int_E [\overline{p_\ell^*}]\cdot\nu_E(u - u_\ell)ds.\square\end{aligned}$$

The local refinement indicators $|\eta_T + \eta_T^*|$ are defined as

$$\begin{aligned}\eta_T &:= \int_T (\beta\cdot p_\ell - \lambda_\ell u_\ell)\overline{e_\ell^*}dx + \sum_{E\in\partial T}\int_E ([p_\ell]\cdot\nu_E)\overline{e_\ell^*}ds,\\ \eta_T^* &:= \int_T (-\beta\cdot\overline{p_\ell^*} - \overline{\lambda_\ell^* u_\ell^*})e_\ell dx + \sum_{E\in\partial T}\int_E ([\overline{p_\ell^*}]\cdot\nu_E)e_\ell ds.\end{aligned}$$

They are only necessary to determine the set of marked edges for refinement.

Utilising the non standard Raviart-Thomas solution of an auxiliary problem leads to a new approach of dual-weighted error estimators.

Lemma 4.3. *Let $q_M \in RT_0(\mathcal{T}_\ell)$ and $q_M^* \in RT_0(\mathcal{T}_\ell)$ be the mixed solutions of the equilibrium conditions*

$$\begin{aligned}-div(q_M) + \beta\cdot q_M &= f_\ell \text{ in } \Omega,\\ -div(q_M^*) - \beta\cdot q_M^* &= f_\ell^* \text{ in } \Omega\end{aligned}$$

with right-hand sides $f_\ell, f_\ell^* \in \mathcal{P}_0(\mathcal{T}_\ell)$ given by $f_{\ell|T} := h_T^{-2}\int_T \lambda_\ell u_\ell$ and $f_{\ell|T}^* := h_T^{-2}\int_T \lambda_\ell^* u_\ell^*$ for $T \in \mathcal{T}_\ell$. Then for the unknown exact errors e_ℓ and e_ℓ^* it holds

$$\begin{aligned}|\lambda - \lambda_\ell| \lesssim \eta_{\ell,DWM} := |&\int_\Omega (p_\ell - q_M)\nabla\overline{e_\ell^*}dx + \int_\Omega (\overline{p_\ell^* - q_M^*})\nabla e_\ell dx\\ &+ \int_\Omega \beta\cdot(p_\ell - q_M)\overline{e_\ell^*}dx - \int_\Omega \beta\cdot(\overline{p_\ell^* - q_M^*})e_\ell dx|\\ &+ h.o.t.\end{aligned}$$

with the higher-order term

$$h.o.t. := |\int_\Omega (f_\ell - \lambda_\ell u_\ell)\overline{e_\ell^*}dx + \int_\Omega (\overline{f_\ell^* - \lambda_\ell^* u_\ell^*})e_\ell dx|.$$

Proof. By the definition of the auxiliary problem for q_M and integration by parts it holds

$$\begin{aligned}\mathrm{Res}_\ell(e_\ell^*) &= \int_\Omega p_\ell \nabla \overline{e_\ell^*} dx + \int_\Omega (\beta \cdot p_\ell - \lambda_\ell u_\ell)\overline{e_\ell^*} dx \\ &= \int_\Omega (p_\ell - q_M)\nabla \overline{e_\ell^*} dx + \int_\Omega \beta \cdot (p_\ell - q_M)\overline{e_\ell^*} dx + \int_\Omega (f_\ell - \lambda_\ell u_\ell)\overline{e_\ell^*} dx.\end{aligned}$$

Using the same argumentation leads to

$$\begin{aligned}\mathrm{Res}_\ell^*(e_\ell) &= \int_\Omega \overline{p_\ell^*} \nabla e_\ell dx + \int_\Omega (-\beta \cdot \overline{p_\ell^*} - \overline{\lambda_\ell^* u_\ell^*}) e_\ell dx \\ &= \int_\Omega (\overline{p_\ell^* - q_M^*}) \nabla e_\ell dx - \int_\Omega \beta \cdot (\overline{p_\ell^* - q_M^*}) e_\ell dx + \int_\Omega (\overline{f_\ell^* - \lambda_\ell^* u_\ell^*}) e_\ell dx. \square\end{aligned}$$

Remark 4.2. Approximating ∇u and $\nabla \overline{u^*}$ by $A(p_\ell)$ and $A(\overline{p_\ell^*})$, using the averaging technique of Section 3, leads to the error estimator

$$\begin{aligned}|\lambda - \lambda_\ell| \lesssim |\int_\Omega (p_\ell - q_M)\nabla(A(\overline{p_\ell^*}) - \overline{p_\ell^*}) dx + \int_\Omega (\overline{p_\ell^* - q_M^*})(A(p_\ell) - p_\ell) dx \\ + \int_\Omega \beta \cdot (p_\ell - q_M)\overline{e_\ell^*} dx - \int_\Omega \beta \cdot (\overline{p_\ell^* - q_M^*}) e_\ell dx|\end{aligned}$$

and the local refinement indicators

$$\begin{aligned}\eta_T := |\int_T (p_\ell - q_M)\nabla(A(\overline{p_\ell^*}) - \overline{p_\ell^*}) dx + \int_T (\overline{p_\ell^* - q_M^*})(A(p_\ell) - p_\ell) dx \\ + \int_T \beta \cdot (p_\ell - q_M)\overline{e_\ell^*} dx - \int_T \beta \cdot (\overline{p_\ell^* - q_M^*}) e_\ell dx|.\end{aligned}$$

The second new error estimator makes use of the ideas of the modern DWR paradigm. The new aspect proposed here is not to use integration by parts to obtain a residual term but to involve an average term and do integration by parts only on that.

Lemma 4.4. *For the unknown exact errors e_ℓ and e_ℓ^* let*

$$\begin{aligned}\mu &:= \int_\Omega (p_\ell - A(p_\ell))\nabla \overline{e_\ell^*} dx + \int_\Omega (-div(A(p_\ell)) + \beta \cdot p_\ell - \lambda_\ell u_\ell)\overline{e_\ell^*} dx, \\ \mu^* &:= \int_\Omega (\overline{p_\ell^*} - A(\overline{p_\ell^*}))\nabla e_\ell dx + \int_\Omega (-div(A(\overline{p_\ell^*})) - \beta \cdot \overline{p_\ell^*} - \overline{\lambda_\ell^* u_\ell^*}) e_\ell dx,\end{aligned}$$

then it holds

$$|\lambda - \lambda_\ell| \lesssim \mu_{\ell,DWA} := |\mu + \mu^*|.$$

Proof. Adding and subtracting an averaging term and using integration by parts on one of them yields

$$\begin{aligned}\mathrm{Res}_\ell(e_\ell^*) &= a(u_\ell, u^* - u_\ell^*) - \lambda_\ell b(u_\ell, u^* - u_\ell^*) \\ &= \int_\Omega (p_\ell - A(p_\ell))\nabla \overline{e_\ell^*} dx + \int_\Omega (-\mathrm{div}(A(p_\ell)) + \beta \cdot p_\ell - \lambda_\ell u_\ell)\overline{e_\ell^*} dx.\end{aligned}$$

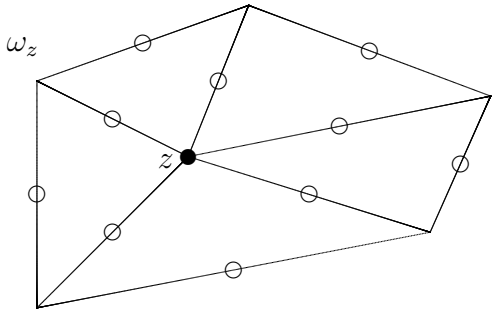

FIGURE 5.1. Interpolation points for the patch ω_z to the node $z \in \mathcal{N}_\ell$.

Analogously it holds

$$\begin{aligned}\mathrm{Res}^*_\ell(e_\ell) &= a(u-u_\ell, u^*_\ell) - \overline{\lambda^*_\ell} b(u-u_\ell, u^*_\ell)\\ &= \int_\Omega (\overline{p^*_\ell} - A(\overline{p^*_\ell}))\nabla e_\ell dx + \int_\Omega (-\mathrm{div}(A(\overline{p^*_\ell})) - \beta\cdot\overline{p^*_\ell} - \overline{\lambda^*_\ell u^*_\ell}) e_\ell dx. \square\end{aligned}$$

Here, the local refinement indicators read $|\mu_T + \mu^*_T|$ with

$$\begin{aligned}\mu_T &:= \int_T (p_\ell - A(p_\ell))\nabla \overline{e^*_\ell} dx + \int_T (-\mathrm{div}(A(p_\ell)) + \beta\cdot p_\ell - \lambda_\ell u_\ell)\overline{e^*_\ell} dx,\\ \mu^*_T &:= \int_T (\overline{p^*_\ell} - A(\overline{p^*_\ell}))\nabla e_\ell dx + \int_T (-\mathrm{div}(A(\overline{p^*_\ell})) - \beta\cdot\overline{p^*_\ell} - \overline{\lambda^*_\ell u^*_\ell}) e_\ell dx.\end{aligned}$$

5. Numerical Experiments

This section is denoted to the numerical experiments. Besides the numerical evidence of reliability and efficiency the stability of the different error estimators for problems with strong convection terms are of special interest.

Since for the dual-weighted error estimators the weight-terms e_ℓ and $\overline{e^*_\ell}$ involve the unknown solutions u and $\overline{u^*}$ these have to be approximated. In the following experiments those functions are approximated by averaging $A(u_\ell) \in P_2(\mathcal{T}_\ell)$ of $u_\ell \in P_1(\mathcal{T}_\ell)$ and $A(\overline{u^*_\ell}) \in P_2(\mathcal{T}_\ell)$ of $\overline{u^*_\ell} \in P_1(\mathcal{T}_\ell)$ on the mesh $\mathcal{T}_\ell$. This is done by nodal-patch wise least square global quadratic polynomial fitting, [ZZ92]. The interpolation points are the midpoints of all edges belonging to the nodal-patch as depicted in Figure 5.1. Evaluating the computed quadratic polynomial for the patch ω_z in the node $z \in \mathcal{N}_\ell$ gives one coefficient for the basis function belonging to z. After all nodal coefficients have been interpolated, the coefficients for the edge basis functions are computed as arithmetic mean of two neighbouring node-values.

The experiments use the adaptive finite element method (AFEM). It generates a sequence of meshes $\mathcal{T}_0, \mathcal{T}_1, \ldots, \mathcal{T}_\ell, \mathcal{T}_{\ell+1}, \ldots$ and associated discrete subspaces

$$V_0 \subsetneq V_1 \subsetneq \ldots \subsetneq V_\ell \subsetneq V_{\ell+1} \subsetneq \ldots \subsetneq V$$

with discrete primal and dual eigenpairs (λ_ℓ, u_ℓ), $(\lambda_\ell^*, u_\ell^*)$. A typical loop from V_ℓ to $V_{\ell+1}$ consists of the steps

$$\text{SOLVE} \to \text{ESTIMATE} \to \text{MARK} \to \text{REFINE}.$$

The implementation of the step SOLVE in the programming language MATLAB in the spirit of [ACF99] is given in Figure 5.2.

The step ESTIMATE involves an appropriate a posteriori error estimator. In the numerical examples below the following error estimators are compared.

$$\begin{aligned}
\eta_\ell &= \sum_{T\in\mathcal{T}} h_T^2 \|\beta\cdot p_\ell - \lambda_\ell u_\ell\|_{L^2(T)}^2 + \sum_{E\subset T} h_E \|[p_\ell]\cdot\nu_E\|_{L^2(E)}^2 \\
&\quad + \sum_{T\in\mathcal{T}} h_T^2 \|-\beta\cdot\overline{p_\ell^*} - \overline{\lambda_\ell^* u_\ell^*}\|_{L^2(T)}^2 + \sum_{E\subset T} h_E \|[\overline{p_\ell^*}]\cdot\nu_E\|_{L^2(E)}^2, \\
\mu_\ell &= \sum_{T\in\mathcal{T}} h_T^2 \|-\operatorname{div}(A(p_\ell)) + \beta\cdot p_\ell - \lambda_\ell u_\ell\|_{L^2(T)}^2 + \|A(p_\ell) - p_\ell\|_{L^2(T)}^2 \\
&\quad + \sum_{T\in\mathcal{T}} h_T^2 \|-\operatorname{div}(A(\overline{p_\ell^*})) - \beta\cdot\overline{p_\ell^*} - \overline{\lambda_\ell^* u_\ell^*}\|_{L^2(T)}^2 + \|A(\overline{p_\ell^*}) - \overline{p_\ell^*}\|_{L^2(T)}^2, \\
\eta_{\ell,\text{reduced}} &= \sum_{E\in\mathcal{E}_\ell} h_E \big\| [p_\ell]\cdot\nu_E\big\|_{L^2(E)}^2 + \sum_{E\in\mathcal{E}_\ell} h_E \big\| \big[\overline{p_\ell^*}\big]\cdot\nu_E\big\|_{L^2(E)}^2, \\
\mu_{\ell,\text{reduced}} &= \sum_{T\in\mathcal{T}_\ell} \|A(p_\ell) - p_\ell\|_{L^2(T)}^2 + \sum_{T\in\mathcal{T}_\ell} \|A(\overline{p_\ell^*}) - \overline{p_\ell^*}\|_{L^2(T)}^2, \\
\eta_{\ell,\text{DWR1}} &= \sum_{T\in\mathcal{T}_\ell} h_T^{3/2} \Big(\|\beta\cdot p_\ell - \lambda_\ell u_\ell\|_{L^2(T)}^2 \\
&\qquad + h_T^{-1} \|[p_\ell]\cdot\nu_E\|_{L^2(\partial T)}^2 \Big)^{1/2} \|[p_\ell^*]\cdot\nu_E\|_{L^2(\partial T)} \\
&\quad + \sum_{T\in\mathcal{T}_\ell} h_T^{3/2} \Big(\|-\beta\cdot\overline{p_\ell^*} - \overline{\lambda_\ell^* u_\ell^*}\|_{L^2(T)}^2 \\
&\qquad + h_T^{-1} \|[p_\ell^*]\cdot\nu_E\|_{L^2(\partial T)}^2 \Big)^{1/2} \|[p_\ell]\cdot\nu_E\|_{L^2(\partial T)}, \\
\eta_{\ell,\text{DWR2}} &= \Big| \sum_{T\in\mathcal{T}_\ell} \int_T (\beta\cdot p_\ell - \lambda_\ell u_\ell)(A(\overline{u_\ell^*}) - \overline{u_\ell^*}) dx \\
&\quad + \sum_{E\in\mathcal{E}} \int_E ([p_\ell]\cdot\nu_E)(A(\overline{u_\ell^*}) - \overline{u_\ell^*}) ds \\
&\quad + \sum_{T\in\mathcal{T}_\ell} \int_T (-\beta\cdot\overline{p_\ell^*} - \overline{\lambda_\ell^* u_\ell^*})(A(u_\ell) - u_\ell) dx \\
&\quad + \sum_{E\in\mathcal{E}} \int_E ([\overline{p_\ell^*}]\cdot\nu_E)(A(u_\ell) - u_\ell) ds \Big|,
\end{aligned}$$

EWP.m

```
function [x,lambda] = EWP(coordinates,elements,dirichlet,k,beta)

A = sparse(size(coordinates,1),size(coordinates,1));
B = sparse(size(coordinates,1),size(coordinates,1));
x = zeros(size(coordinates,1),1);

for j = 1:size(elements,1)
    A(elements(j,:),elements(j,:)) = A(elements(j,:),elements(j,:))+...
      stima(coordinates(elements(j,:),:),beta);
    B(elements(j,:),elements(j,:)) = B(elements(j,:),elements(j,:))+...
      det([ones(1,3);coordinates(elements(j,:),:)'])*(ones(3)+eye(3))/24;
end

freeNodes = setdiff(1:size(coordinates,1),unique(dirichlet));
[V,D] = eigs(A(freeNodes,freeNodes),B(freeNodes,freeNodes),k,'sm');
x(freeNodes) = V(:,1);lambda = D(1,1);

function stima=stima(vertices,b)
P = [ones(1,3);vertices'];
Q = P\[zeros(1,2);eye(2)];
stima = det(P)*(Q*Q'+ Q*beta*ones(1,3)/3)/2;
```

FIGURE 5.2. 17 Lines of Matlab for solving a non-symmetric eigenvalue problem.

$$\eta_{\ell,\mathrm{DWM}} = |\int_\Omega (p_\ell - q_M)\nabla(A(\overline{p_\ell^*}) - \overline{p_\ell^*})dx + \int_\Omega (\overline{p_\ell^* - q_M^*})(A(p_\ell) - p_\ell)dx$$
$$+ \int_\Omega \beta\cdot(p_\ell - q_M)(A(\overline{u_\ell^*}) - \overline{u_\ell^*})dx - \int_\Omega \beta\cdot(\overline{p_\ell^* - q_M^*})(A(u_\ell) - u_\ell)dx|,$$
$$\mu_{\ell,\mathrm{DWA}} = |\int_\Omega (p_\ell - A(p_\ell))(A(\overline{p_\ell^*}) - \overline{p_\ell^*})dx$$
$$+ \int_\Omega (-\mathrm{div}(A(p_\ell)) + \beta\cdot p_\ell - \lambda_\ell u_\ell)(A(\overline{u_\ell^*}) - \overline{u_\ell^*})dx$$
$$+ \int_\Omega (\overline{p_\ell^*} - A(\overline{p_\ell^*}))(A(p_\ell) - p_\ell)dx$$
$$+ \int_\Omega (-\mathrm{div}(A(\overline{p_\ell^*})) - \beta\cdot\overline{p_\ell^*} - \overline{\lambda_\ell^* u_\ell^*})(A(u_\ell) - u_\ell)dx|.$$

In [BE03] an alternative way of computing the estimator η_{DWR2} based on nodal values is presented. The analysis of this error estimator makes use of a special interpolation operator for quadrilateral meshes. This interpolation operator considers the nodal values as values for a higher-order P_2 basis on a coarser grid. Because of the use of the special properties of the interpolation operator this estimator can not be applied to the more general structured triangular meshes used in this paper.

In order to compare the different non-weighted and dual-weighted error estimators, the efficiency indices of all estimators for different convection parameters β are compared based on three different sequences

of meshes. The first sequence consists on uniform (red) refined meshes, the second sequence consists on perturbed adaptive meshes generated by the altered AFEM given in Algorithm 5.1, c.f. [CB02]. For the mesh-adaptivity the residual estimator η_ℓ is chosen. In addition the nodes of the mesh are perturbed in order to avoid super-convergence phenomena due to mesh symmetries. Third, all error estimators are compared on sequences of adaptive meshes which are created by the corresponding error estimators during the AFEM loop.

Algorithm 5.1. Input: Coarse mesh $\mathcal{T}_0$.
SOLVE: Solve the discrete eigenvalue problem on the mesh $\mathcal{T}_\ell$ in order to obtain a primal discrete eigenpair (λ_ℓ, u_ℓ) and a corresponding dual discrete eigenpair $(\lambda_\ell^*, u_\ell^*)$.
ESTIMATE: Calculate all error estimators based on the primal and dual discrete eigenpairs (λ_ℓ, u_ℓ) and $(\lambda_\ell^*, u_\ell^*)$, but only the refinement indicators of the residual error estimator η_ℓ.
MARK: Mark all edges of triangles accordingly to the local refinement indicators of the residual estimator η_ℓ with a bulk criterion. Let $\mathcal{M}_\ell$ be the smallest possible set of triangles, such that

$$\frac{1}{2}\sum_{T\in\mathcal{T}_\ell}\eta_{T,\ell} \leq \sum_{T\in\mathcal{M}_\ell}\eta_{T,\ell}.$$

REFINE: Refine the mesh using the red-green-blue algorithm [Car04] and perturb the resulting mesh $\mathcal{T}_{\ell+1}$ as follows. Each new node $z \in \mathcal{N}_{\ell+1}\backslash\mathcal{N}_\ell$ is a midpoint of an edge $E_z \in \mathcal{E}_\ell$, therefore perturb each node z along the edge E_z at random around the midpoint within the range of $h_E/5$. Afterwards perturb all inner nodes $z \in \mathcal{N}_{\ell+1}$ at random within a ball with radius $r_z = (5 \cdot 2^{\ell+1})^{-1}$. Set $\ell = \ell + 1$ and continue with SOLVE.
Output: Perturbed adaptive mesh $\mathcal{T}_\ell$ and computed discrete primal and dual discrete eigenpairs (λ_ℓ, u_ℓ) and (λ_ℓ, u_ℓ), as well as values for all error estimators on each level ℓ.

In order to fix an eigenvalue λ_0 of interest for all numerical experiments, notice that for the model problem there exists an real eigenvalue λ_0 such that for all distinct eigenvalues λ_j it holds

$$\lambda_0 \leq \operatorname{Re}\lambda_j \qquad j = 1, 2, \ldots$$

For this eigenvalue there exists a corresponding eigenfunction u_0 such that $u_0 > 0$ in Ω. The eigenvalue λ_0 is simple, [Eva00, Section 6.5].

The numerical examples are done for three different domains. The first one is a convex domain, the unit square, while the other two have re-entrant corners, namely the L shaped and slit domain. In general the numerical experiments show that the efficiency indices for some dual-weighted error estimators are near the expected value $1/(2|b(u, u^*)|)$ while the ones of the non-weighted error estimators result in higher indices. Moreover the numerical examples verify the theoretical findings

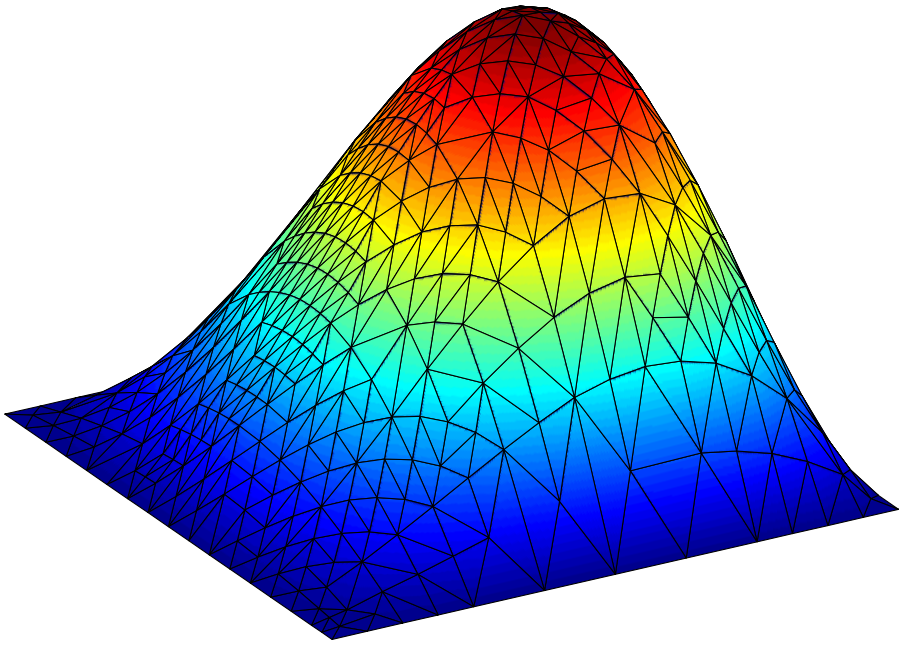

FIGURE 5.3. Primal discrete solution for $\beta = (3,0)^T$ on adaptively refined meshes generated by η_ℓ on the unit square with about 500 nodes.

that for the non-weighted error estimators the increase of the convection coefficient results in an increase of the efficiency index which is not preferred. In addition, this change seems to be growing not proportional to the change of the coefficient which is even worse. Therefore, for convection dominated problems, it is necessary to consider error estimators which are independent of the size of the convection coefficient. The numerical experiments indicate that the efficiency index of the $\eta_{\ell,\mathrm{DWR2}}$, the $\eta_{\ell,\mathrm{DWM}}$ and the $\mu_{\ell,\mathrm{DWA}}$ error estimators are relatively independent of the convection term.

In the numerical examples the convection parameter is chosen out of $\beta \in \{(1,0)^T, (2,0)^T, (3,0)^T\}$. In order to calculate any eigenvalue error $|\lambda - \lambda_\ell|$, the exact eigenvalue, which strongly depends on the chosen convection parameter $\beta \in \mathbb{R}^2$, is thereby replaced by a approximation $\tilde{\lambda}$ with high accuracy. The values for $\tilde{\lambda}$ and $2|b(u,u^*)|$, the asymptotic constant involved in Lemma 2.1, are obtained by Aitken extrapolation of the sequences $(\lambda_\ell)_\ell$ and $(2|b(u_\ell,u_\ell^*)|)_\ell$ on uniform meshes.

5.1. **Unit Square.** As first example consider the non-symmetric eigenvalue problem

$$-\Delta u + \beta \cdot \nabla u = \lambda u \quad \text{in } \Omega \qquad \text{and} \qquad u = 0 \quad \text{on } \partial\Omega$$

on the unit square $\Omega = [0,1] \times [0,1]$. The discrete primal and dual solutions are displayed in Figures 5.3 and 5.4.

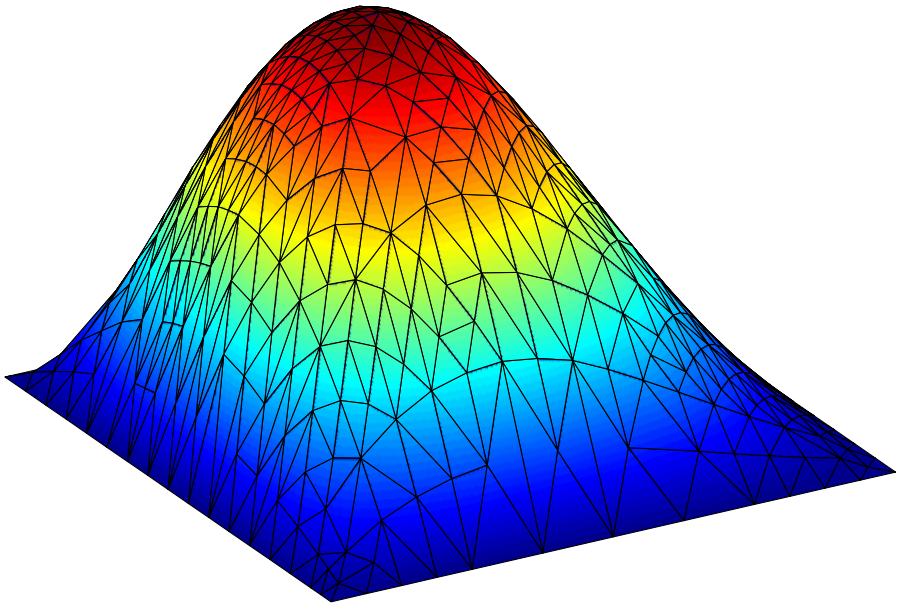

FIGURE 5.4. Dual discrete solution for $\beta = (3, 0)^T$ on adaptively refined meshes generated by η_ℓ on the unit square with about 500 nodes.

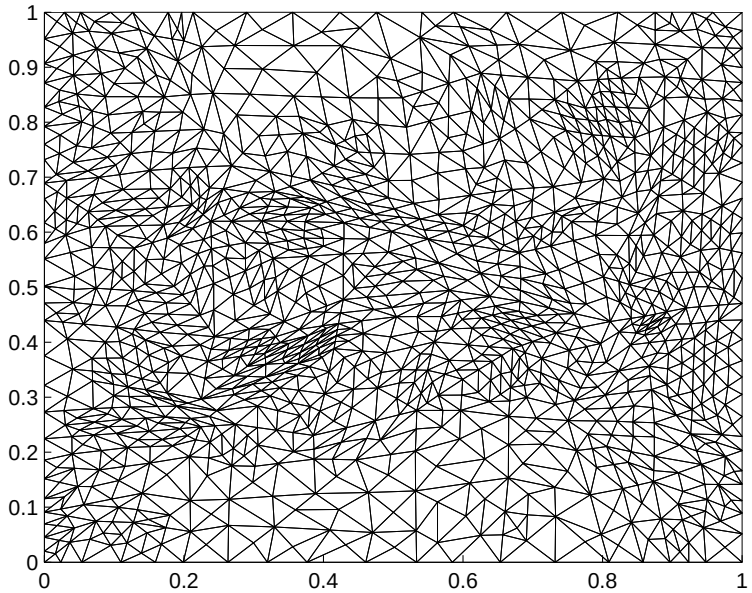

FIGURE 5.5. Perturbed mesh, with about 1262 nodes, generated by Algorithm 5.1 with $\beta = (3, 0)^T$ for the unit square.

Because the domain is convex, uniform refinement results in optimal convergence rates. However using different sequences of adaptive meshes verifies whether all error estimators are reliable and efficient. Concerning the experiments on uniform meshes, as shown in Figures 5.6 and 5.7, all error estimators indicate reliability and efficiency due to the fact, that the efficiency indices stabilise towards a stationary value. It is remarkable that the averaging error estimator μ_ℓ and it's reduced error estimator $\mu_{\ell,\text{reduced}}$ seem to be asymptotically identical, which shows that the additional volumetric part is of higher-order as proven. Moreover it can be seen that the efficiency indices of the non-weighted error estimators grow depending on the convection coefficient β. On the other hand the dual-weighted error estimator $\eta_{\ell,\text{DWR2}}$ and the new proposed estimators $\eta_{\ell,\text{DWM}}$ and $\mu_{\ell,\text{DWA}}$ are rather independent of the norm of the convection coefficient. In general the dual-weighted error estimators, except the estimator $\eta_{\ell,\text{DWR1}}$, have efficiency indices close to $2|b(u,u^*)|$ which is considered as exact. The different values for $2|b(u,u^*)|$ are indicated by the shorter horizontal lines. The residual error estimator η_ℓ and $\eta_{\ell,\text{reduced}}$ show large indices which is not desirable in practical applications.

For the sequence of perturbed adaptive meshes of Algorithm 5.1 the behaviour of the error estimators is similar to the previous case. In Figure 5.5 one mesh of the sequence with 1262 nodes is pictured. In contrast to uniform meshes, the averaging error estimators μ_ℓ and $\mu_{\ell,\text{reduced}}$ are not asymptotic identical, which is shown in Figure 5.8. This is due to the loss of super-convergence phenomena on unstructured meshes. The dual-weighted error estimators show to be less dependent on the convection coefficient as displayed in Figure 5.9. Among those the $\mu_{\ell,\text{DWA}}$ error estimator seems to be nearly independent of any change in the convection coefficient. Again the non-weighted error estimators strongly depend on the norm of β and show large indices.

For sequences of meshes generated by the AFEM using the corresponding refinement indicators, the efficiency indices for the non-weighted error estimators are displayed in Figure 5.10 and those of the dual-weighted error estimators in Figure 5.11. In comparison to the results for perturbed meshes the indices for $\beta = (3,0)^T$ are less stable, which indicates some super-convergence or instability phenomena, since the symmetry is destroyed in the case of perturbed meshes. Besides that, all error estimators show numerically optimal convergence rates of $O(h^2)$. Again the efficiency indices of the non-weighted error estimators are highly depended on changes of the convection coefficient, while the one of the dual-weighted error estimators are less influenced by that. The new proposed $\mu_{\ell,\text{DWA}}$ error estimator seems to be numerically independent of any change of β.

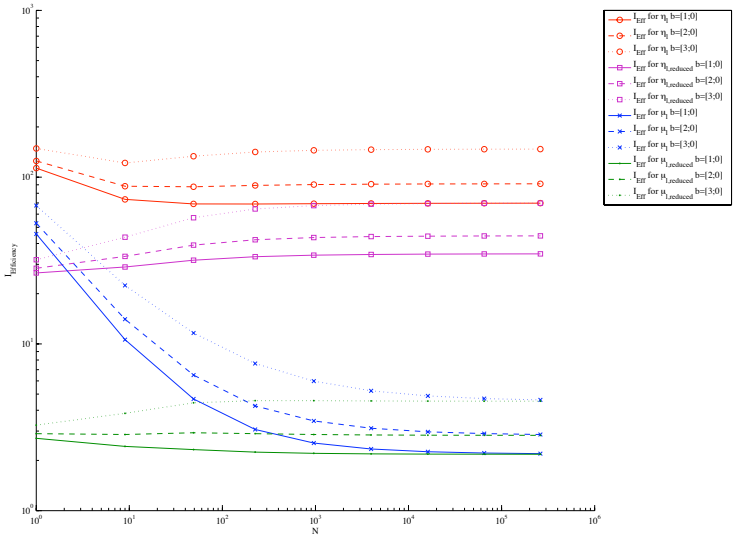

FIGURE 5.6. Efficiency indices for the non-weighted estimators η_ℓ, $\eta_{\ell,\text{reduced}}$, μ_ℓ, $\mu_{\ell,\text{reduced}}$, with convection coefficients $\beta = (1,0)^T$, $\beta = (2,0)^T$ and $\beta = (3,0)^T$ for uniform meshes on the unit square.

The corresponding eigenvalue errors in Figure 5.12 show optimal convergence rates for uniform and adaptive meshes. However the eigenvalue error is of different size as shown in Figure 5.13 with $\beta = (10,0)^T$. Here the proposed $\mu_{\ell,\text{DWA}}$ error estimator performs better than the $\eta_{\ell,\text{DWR2}}$ which produces comparable good efficiency indices. The smallest error, even below the one for uniform meshes, shows the $\eta_{\ell,\text{DWR1}}$, but this estimator does not result in small efficiency indices. Therefore for convection dominated problems the DWA results in the best combination of small error and accurate efficiency indices.

5.2. **L shape.** As second example consider the non-symmetric eigenvalue problem

$$-\Delta u + \beta \cdot \nabla u = \lambda u \quad \text{in } \Omega \qquad \text{and} \qquad u = 0 \quad \text{on } \partial\Omega$$

on the L shaped domain $\Omega = ([-1,1] \times [-1,1]) \backslash ([0,1] \times [0,-1])$. The primal and dual solutions for adaptive meshes generated by the AFEM, based on the residual error estimator η_ℓ, are shown in Figures 5.14 and 5.15.

In contrast to the previous example, adaptive refinement is necessary to obtain numerically optimal convergence rates close to $O(h^2)$, which is due to the singularity of the first eigenfunction at the re-entrant corner. In Figure 5.17 it is shown that uniform refinement results in

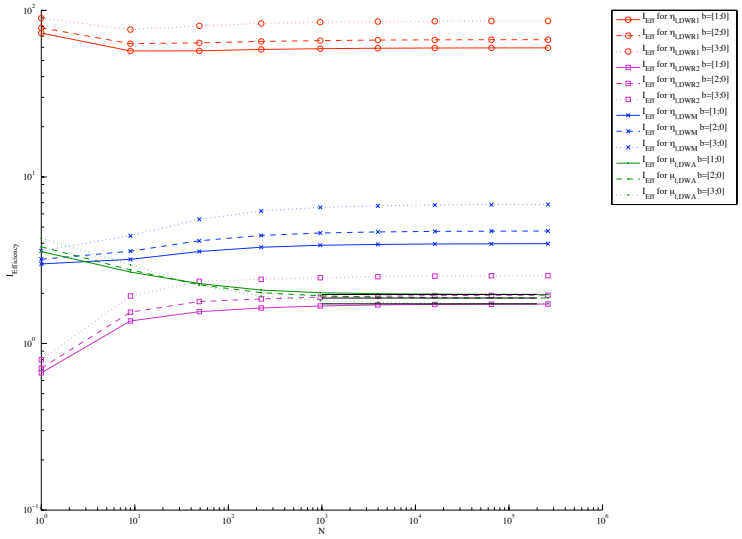

FIGURE 5.7. Efficiency indices for the dual-weighted estimators $\eta_{\ell,\mathrm{DWR1}}$, $\eta_{\ell,\mathrm{DWR2}}$, $\eta_{\ell,\mathrm{DWM}}$ and $\mu_{\ell,\mathrm{DWA}}$ with convection coefficients $\beta = (1,0)^T$, $\beta = (2,0)^T$ and $\beta = (3,0)^T$ for uniform meshes on the unit square.

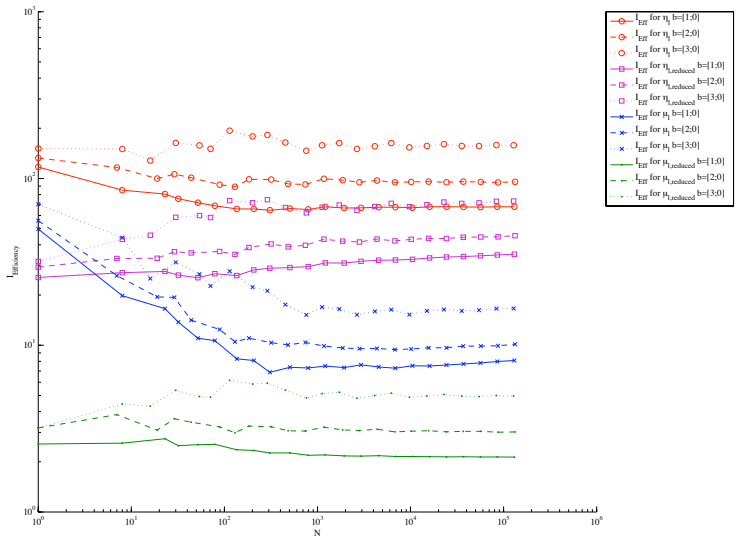

FIGURE 5.8. Efficiency indices for the non-weighted estimators η_ℓ, $\eta_{\ell,\mathrm{reduced}}$, μ_ℓ, $\mu_{\ell,\mathrm{reduced}}$, with convection coefficients $\beta = (1,0)^T$, $\beta = (2,0)^T$ and $\beta = (3,0)^T$ for a sequence of perturbed meshes generated by Algorithm 5.1 on the unit square.

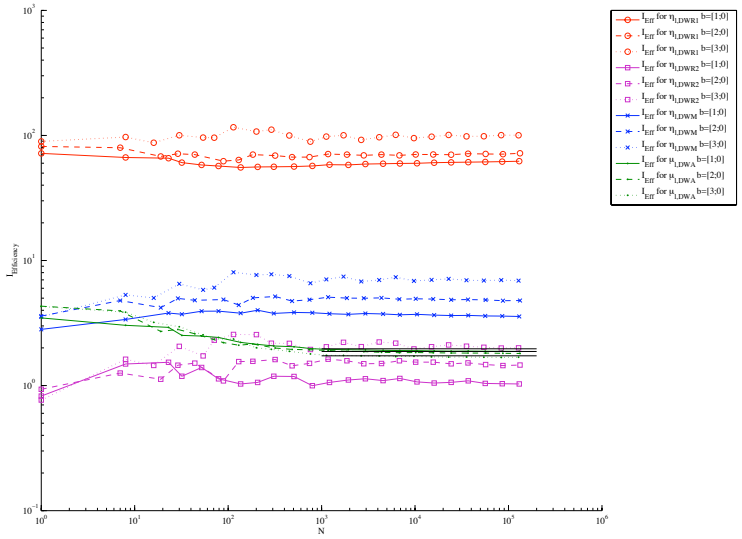

FIGURE 5.9. Efficiency indices for the dual-weighted estimators $\eta_{\ell,\mathrm{DWR1}}$, $\eta_{\ell,\mathrm{DWR2}}$, $\eta_{\ell,\mathrm{DWM}}$ and $\mu_{\ell,\mathrm{DWA}}$ with convection coefficients $\beta = (1,0)^T$, $\beta = (2,0)^T$ and $\beta = (3,0)^T$ for a sequence of perturbed meshes generated by Algorithm 5.1 on the unit square.

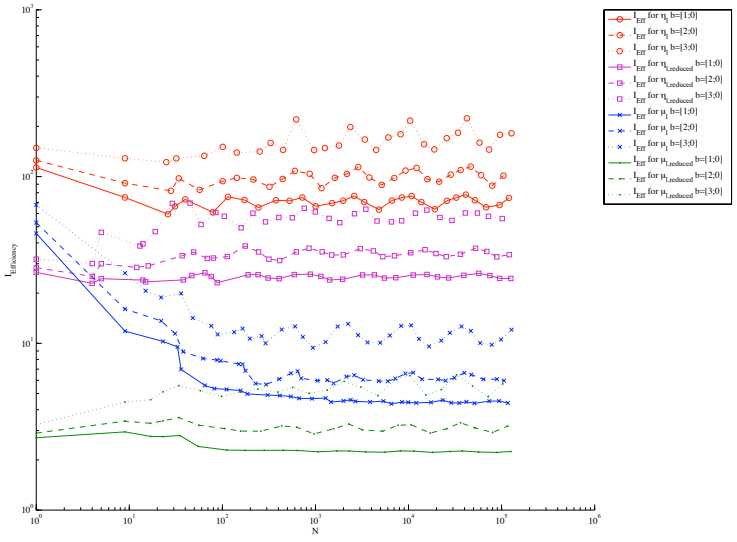

FIGURE 5.10. Efficiency indices for the non-weighted estimators η_ℓ, $\eta_{\ell,\mathrm{reduced}}$, μ_ℓ, $\mu_{\ell,\mathrm{reduced}}$, with convection coefficients $\beta = (1,0)^T$, $\beta = (2,0)^T$ and $\beta = (3,0)^T$ for sequences of meshes generated by the corresponding refinement indicators on the unit square.

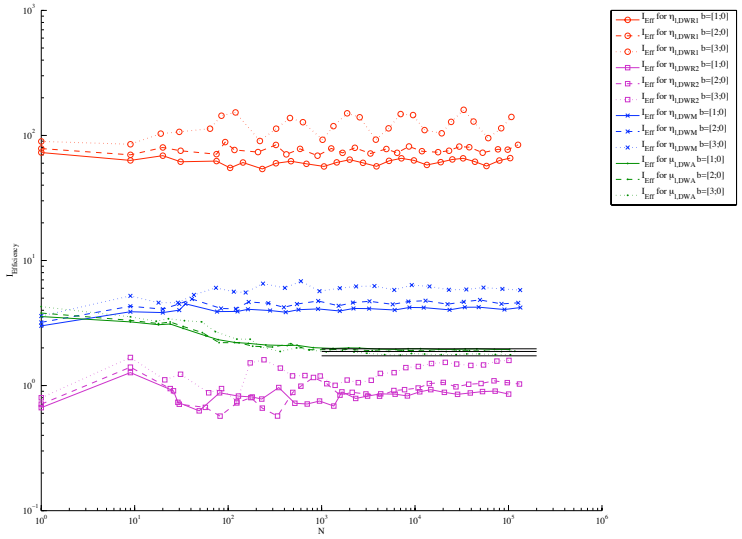

FIGURE 5.11. Efficiency indices for the dual-weighted estimators $\eta_{\ell,\mathrm{DWR1}}$, $\eta_{\ell,\mathrm{DWR2}}$, $\eta_{\ell,\mathrm{DWM}}$ and $\mu_{\ell,\mathrm{DWA}}$ with convection coefficients $\beta = (1,0)^T$, $\beta = (2,0)^T$ and $\beta = (3,0)^T$ for sequences of meshes generated by the corresponding refinement indicators on the unit square.

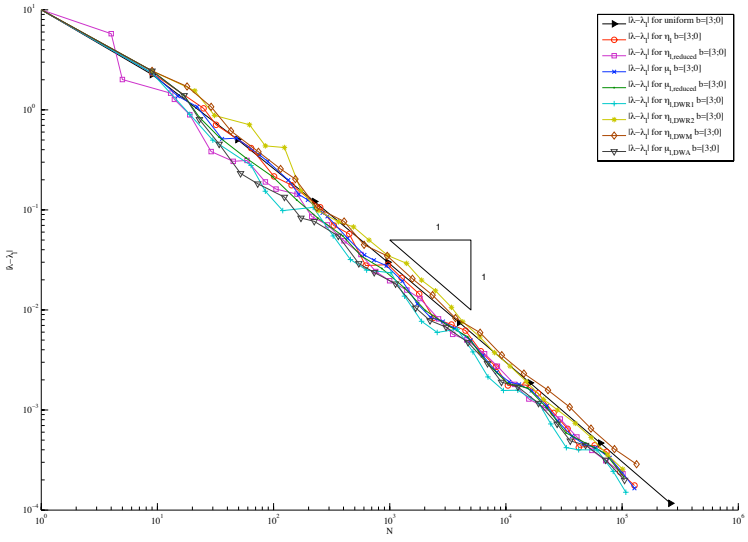

FIGURE 5.12. Eigenvalue errors with $\beta = (3,0)^T$ for a uniform mesh and adaptive meshes generated by η_ℓ, $\eta_{\ell,\mathrm{reduced}}$, μ_ℓ, $\mu_{\ell,\mathrm{reduced}}$, $\eta_{\ell,\mathrm{DWR1}}$, $\eta_{\ell,\mathrm{DWR2}}$, $\eta_{\ell,\mathrm{DWM}}$ and $\mu_{\ell,\mathrm{DWA}}$ on the unit square.

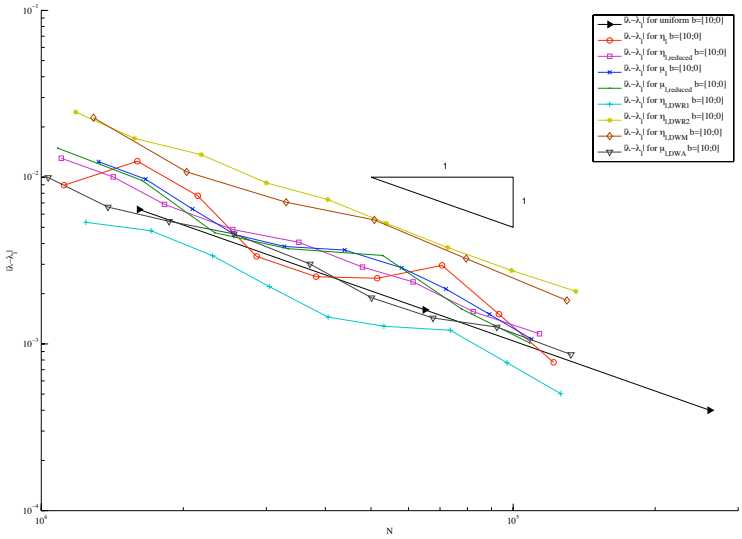

FIGURE 5.13. Eigenvalue errors with $\beta = (10, 0)^T$ for a uniform mesh and adaptive meshes generated by η_ℓ, $\eta_{\ell,\text{reduced}}$, μ_ℓ, $\mu_{\ell,\text{reduced}}$, $\eta_{\ell,\text{DWR1}}$, $\eta_{\ell,\text{DWR2}}$, $\eta_{\ell,\text{DWM}}$ and $\mu_{\ell,\text{DWA}}$ on the unit square.

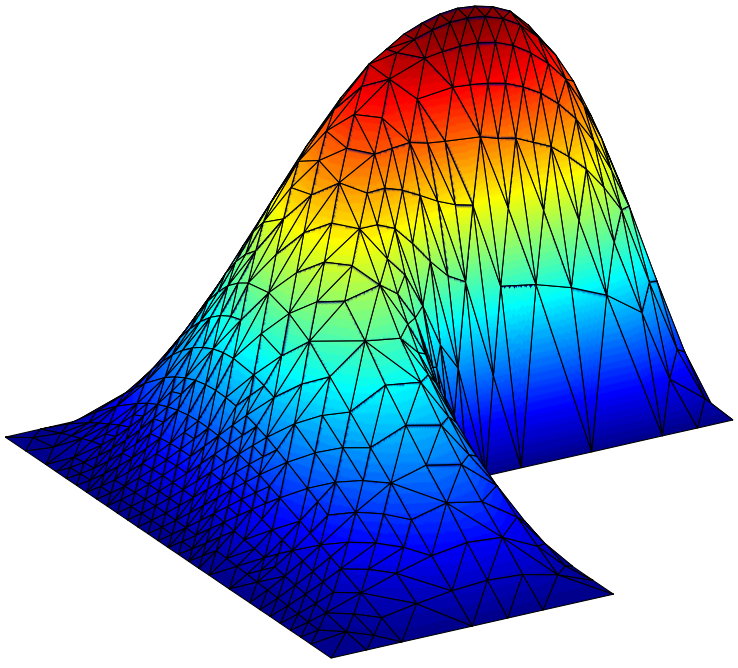

FIGURE 5.14. Primal discrete solution for $\beta = (3, 0)^T$ on adaptively refined meshes generated by η_ℓ on the L shaped domain with about 500 nodes.

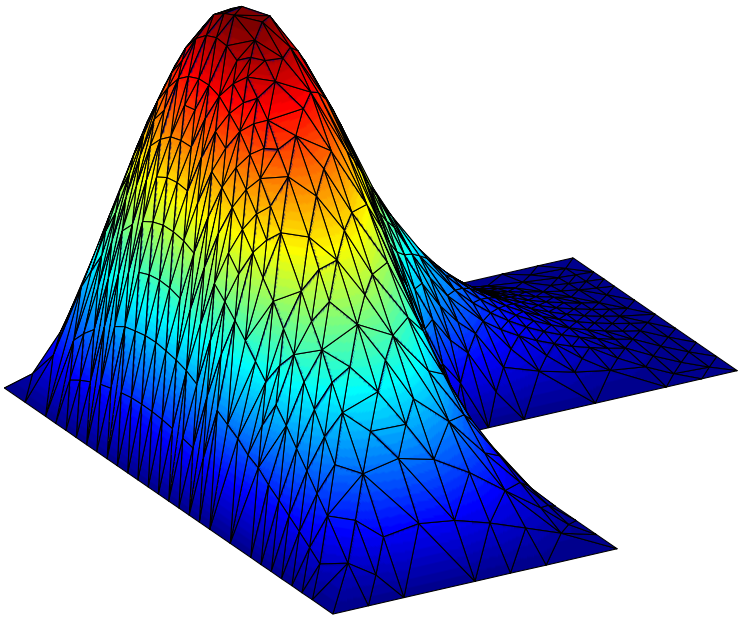

FIGURE 5.15. Dual discrete solution for $\beta = (3,0)^T$ on adaptively refined meshes generated by η_ℓ on the L shaped domain with about 500 nodes.

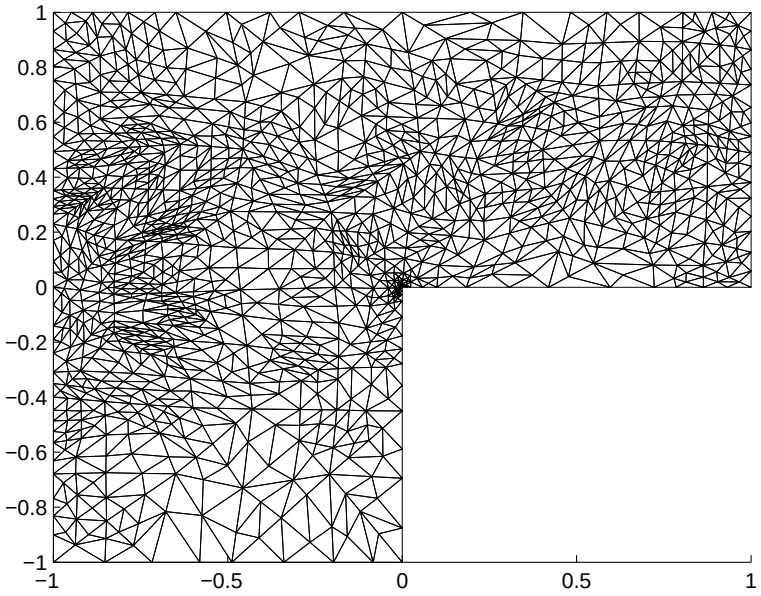

FIGURE 5.16. Perturbed mesh, with 1314 nodes, generated by Algorithm 5.1 with $\beta = (3,0)^T$ for the L shaped domain.

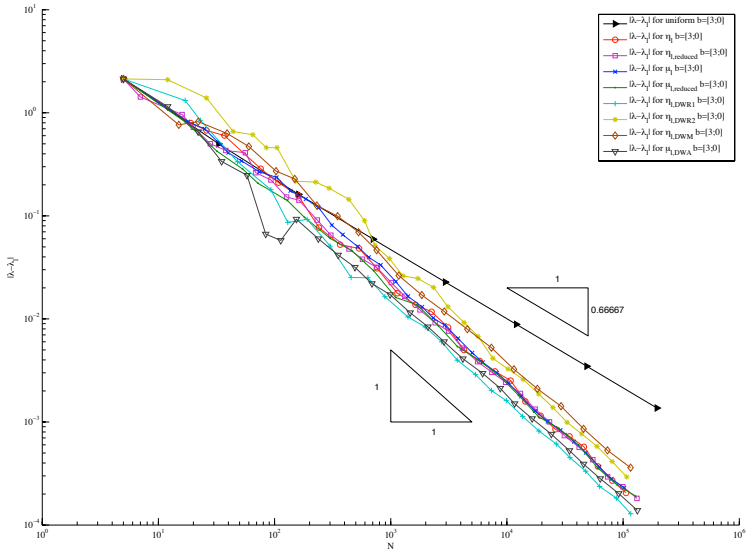

FIGURE 5.17. Eigenvalue errors with $\beta = (3,0)^T$ for a uniform mesh and adaptive meshes generated by η_ℓ, $\eta_{\ell,\text{reduced}}$, μ_ℓ, $\mu_{\ell,\text{reduced}}$, $\eta_{\ell,\text{DWR1}}$, $\eta_{\ell,\text{DWR2}}$, $\eta_{\ell,\text{DWM}}$ and $\mu_{\ell,\text{DWA}}$ on the L shaped domain.

poorer convergence rate of about $O(h^{4/3})$, while all adaptive meshes result in numerically optimal convergence rates.

The experiments for uniform meshes in Figure 5.18 indicate that the non-weighted error estimators are asymptotically independent of β. This phenomenon is due to the suboptimal convergence for uniform meshes and cannot be applied to adaptive meshes. Figure 5.19 shows that for uniform meshes the $\eta_{\ell,\text{DWR2}}$ error estimator is not reliable, because the efficiency index does not stabilise but decreases monotonously. This is due to the fact, that the weights are approximated with averaging techniques which seems to be not sufficient at the re-entrant corner due to the loss of regularity. Therefore it is remarkable that the new proposed $\mu_{\ell,\text{DWA}}$ error estimator is nevertheless numerically reliable. This indicates that for the $\mu_{\ell,\text{DWA}}$ estimator the accuracy of the weights is less important than for the $\eta_{\ell,\text{DWR2}}$ estimator.

As in the previous example the error estimators are all reliable and efficient on perturbed adaptive meshes produced by Algorithm 5.1 and result in optimal convergence rates. A perturbed adaptive mesh for the L shaped domain with 1314 nodes is shown in Figure 5.16. Figure 5.20 shows stronger dependence of the efficiency indices of the non-weighted error estimators on β than the dual-weighted error estimators, as shown in Figure 5.21. As before the dual-weighted error estimators $\eta_{\ell,\text{DWR2}}$,

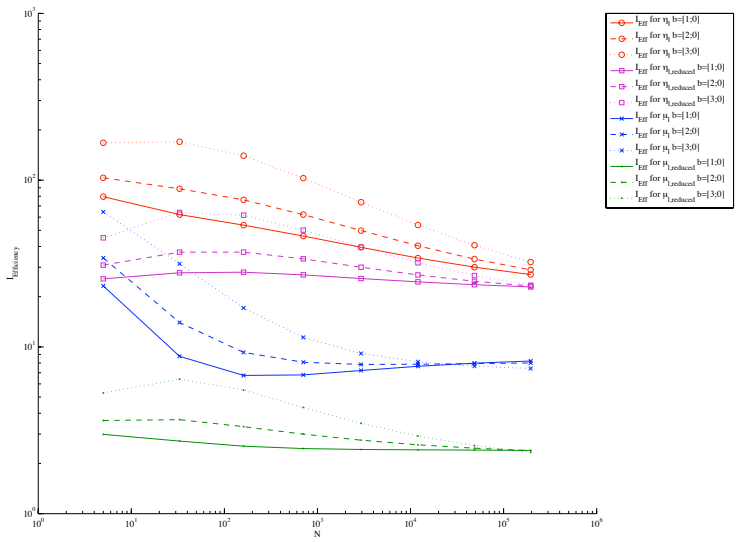

FIGURE 5.18. Efficiency indices for the non-weighted estimators η_ℓ, $\eta_{\ell,\text{reduced}}$, μ_ℓ, $\mu_{\ell,\text{reduced}}$, with convection coefficients $\beta = (1,0)^T$, $\beta = (2,0)^T$ and $\beta = (3,0)^T$ for uniform meshes on the L shaped domain.

$\eta_{\ell,\text{DWM}}$ and $\mu_{\ell,\text{DWA}}$ produce independent of β efficiency indices close to the expected values indicated by the horizontal lines.

In the case of adaptive meshes, all error estimators result in optimal convergence rates as shown in Figure 5.17. Figures 5.22 and 5.23 indicate that the dual-weighted error estimators are in general less dependent on the convection coefficient β. In contrast to the previous examples the efficiency indices of the $\mu_{\ell,\text{DWA}}$ estimator is closer to $2|b(u,u^*)|$ than the $\eta_{\ell,\text{DWR2}}$. One interesting observation is that different error estimators lead to different structured meshes as shown in Figure 5.24.

5.3. **Slit.** As last example consider the non-symmetric eigenvalue problem

$$-\Delta u + \beta \cdot \nabla u = \lambda u \quad \text{in } \Omega \qquad \text{and} \qquad u = 0 \quad \text{on } \partial\Omega$$

on the slit domain $\Omega = ([-1,1] \times [-1,1]) \backslash ([0,1] \times \{0\})$. The primal and dual eigenfunctions on adaptive meshes are shown in Figures 5.25 and 5.26. As in the previous example adaptive refinement results in optimal convergence rates $O(h^2)$, whereas uniform refinement results in convergence of only $O(h)$, due to the corner singularity, which is shown in Figure 5.28.

As in the previous example, Figure 5.30 shows that for uniform meshes the $\eta_{\ell,\text{DWR2}}$ error estimator is not reliable due to the loss of

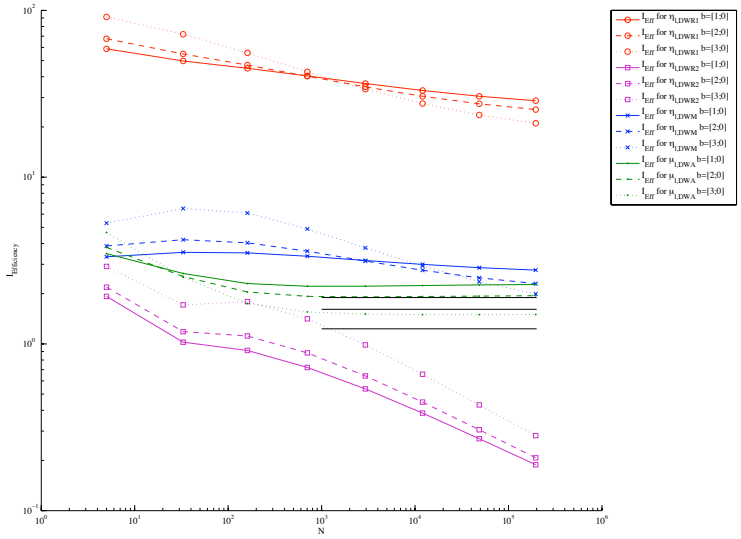

FIGURE 5.19. Efficiency indices for the dual-weighted estimators $\eta_{\ell,\mathrm{DWR1}}$, $\eta_{\ell,\mathrm{DWR2}}$, $\eta_{\ell,\mathrm{DWM}}$ and $\mu_{\ell,\mathrm{DWA}}$ with convection coefficients $\beta = (1,0)^T$, $\beta = (2,0)^T$ and $\beta = (3,0)^T$ for uniform meshes on the L shaped domain.

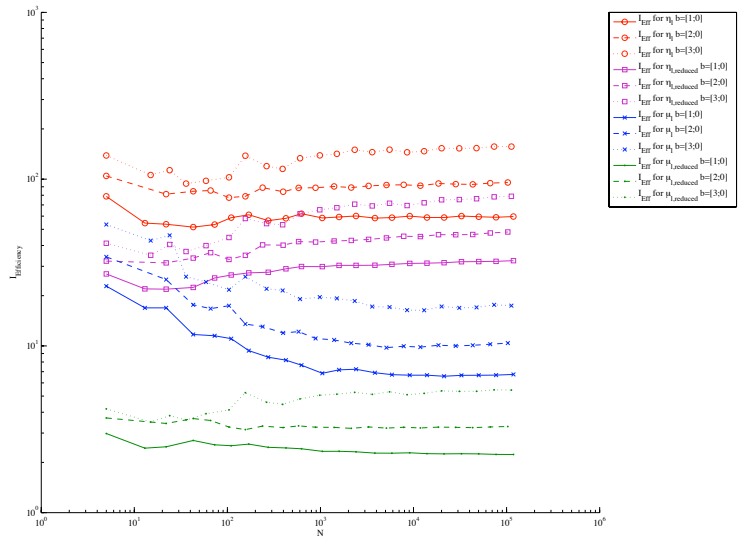

FIGURE 5.20. Efficiency indices for the non-weighted estimators η_ℓ, $\eta_{\ell,\mathrm{reduced}}$, μ_ℓ, $\mu_{\ell,\mathrm{reduced}}$, with convection coefficients $\beta = (1,0)^T$, $\beta = (2,0)^T$ and $\beta = (3,0)^T$ for a sequence of perturbed meshes generated by Algorithm 5.1 on the L shaped domain.

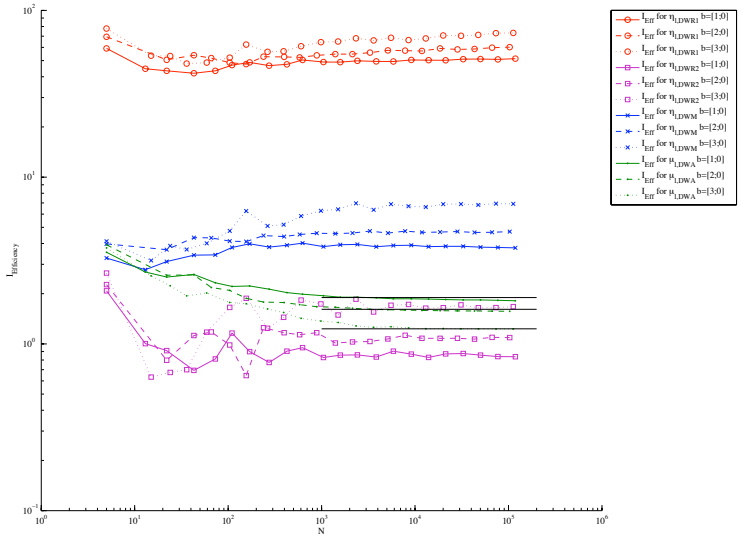

FIGURE 5.21. Efficiency indices for the dual-weighted estimators $\eta_{\ell,\mathrm{DWR1}}$, $\eta_{\ell,\mathrm{DWR2}}$, $\eta_{\ell,\mathrm{DWM}}$ and $\mu_{\ell,\mathrm{DWA}}$ with convection coefficients $\beta = (1,0)^T$, $\beta = (2,0)^T$ and $\beta = (3,0)^T$ for a sequence of perturbed meshes generated by Algorithm 5.1 on the L shaped domain.

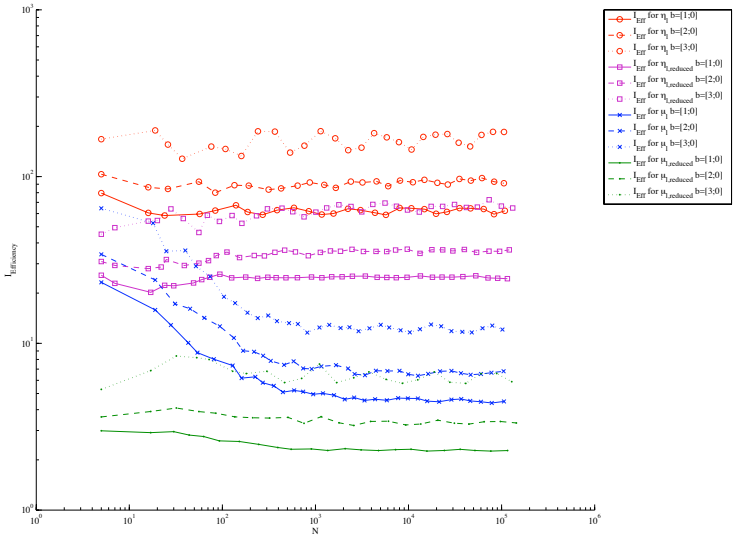

FIGURE 5.22. Efficiency indices for the non-weighted estimators η_ℓ, $\eta_{\ell,\mathrm{reduced}}$, μ_ℓ, $\mu_{\ell,\mathrm{reduced}}$, with convection coefficients $\beta = (1,0)^T$, $\beta = (2,0)^T$ and $\beta = (3,0)^T$ for sequences of meshes generated by the corresponding refinement indicators on the L shaped domain.

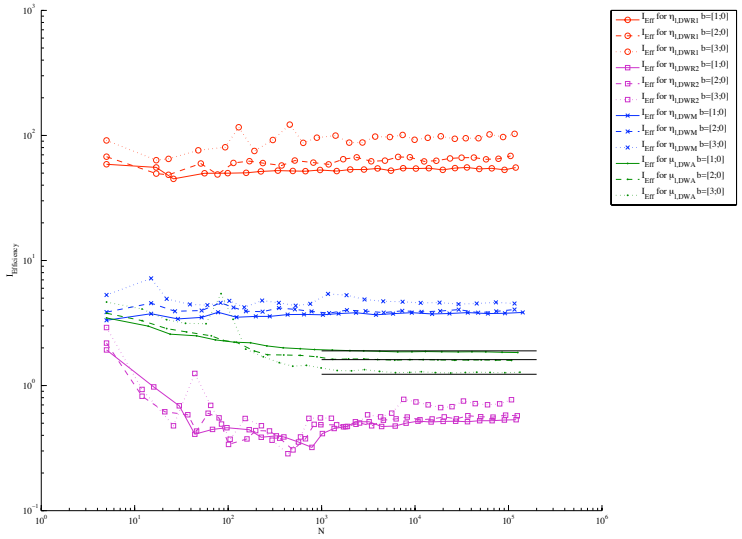

FIGURE 5.23. Efficiency indices for the dual-weighted estimators $\eta_{\ell,\mathrm{DWR1}}$, $\eta_{\ell,\mathrm{DWR2}}$, $\eta_{\ell,\mathrm{DWM}}$ and $\mu_{\ell,\mathrm{DWA}}$ with convection coefficients $\beta = (1,0)^T$, $\beta = (2,0)^T$ and $\beta = (3,0)^T$ for sequences of meshes generated by the corresponding refinement indicators on the L shaped domain.

regularity. Again the new proposed $\mu_{\ell,\mathrm{DWA}}$ error estimator shows to be numerically reliable.

All error estimators are reliable and efficient on perturbed adaptive meshes produced by Algorithm 5.1 and result in optimal convergence rates. A perturbed adaptive mesh for the slit domain with 1465 nodes is shown in Figure 5.27. Figures 5.31 and 5.32 show that the efficiency indices of the non-weighted error estimators depend on β while those of the dual-weighted error estimators do not. As for the other experiments the dual-weighted error estimators $\eta_{\ell,\mathrm{DWR2}}$, $\eta_{\ell,\mathrm{DWM}}$ and $\mu_{\ell,\mathrm{DWA}}$ produce independent of β efficiency indices close to the expected values indicated by the horizontal lines.

Figures 5.33 and 5.34 indicate that for adaptive meshes the dual-weighted error estimators are less dependent on the convection coefficient β than the non-weighted. Again the efficiency indices of $\eta_{\ell,\mathrm{DWR2}}$ and $\mu_{\ell,\mathrm{DWA}}$ are very close to $2|b(u,u^*)|$. The different structured adaptive meshes for the different error estimators are shown in Figure 5.35.

ACKNOWLEDGEMENTS

The authors would like to thank V. Mehrmann and A. Miedlar from TU Berlin and R. Rannacher from University of Heidelberg for inspiring discussions. The work of the two authors was supported by the

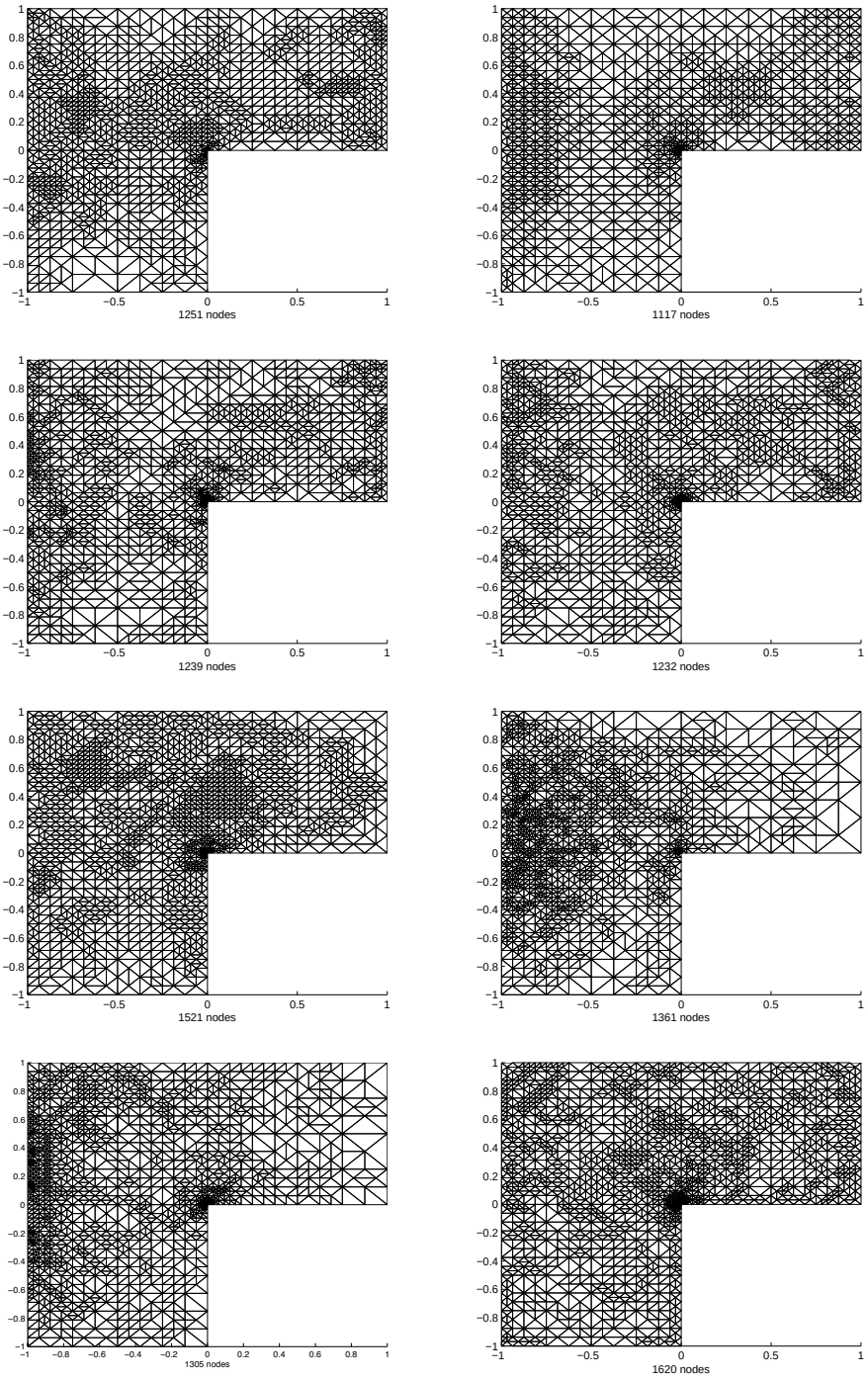

FIGURE 5.24. Meshes with $\beta = (3,0)^T$ generated by the estimators (from left to right and top to bottom) η_ℓ, $\eta_{\ell,\text{reduced}}$, μ_ℓ, $\mu_{\ell,\text{reduced}}$, $\eta_{\ell,\text{DWR1}}$, $\eta_{\ell,\text{DWR2}}$, $\eta_{\ell,\text{DWM}}$ and $\mu_{\ell,\text{DWA}}$ on the L shaped domain with about 1000 up to 1500 nodes.

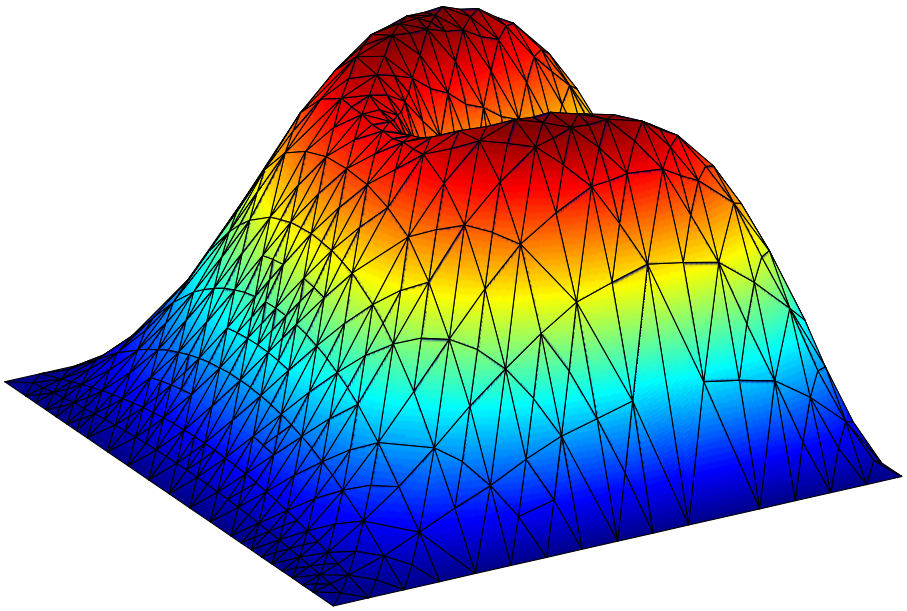

FIGURE 5.25. Primal discrete solution for $\beta = (3,0)^T$ on adaptively refined meshes generated by η_ℓ on the slit domain with about 500 nodes.

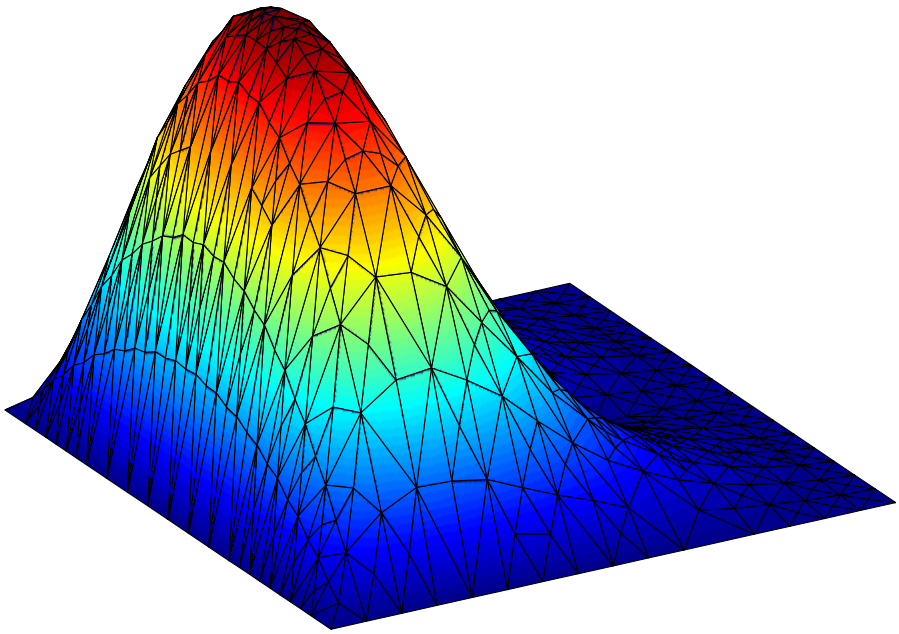

FIGURE 5.26. Dual discrete solution for $\beta = (3,0)^T$ on adaptively refined meshes generated by η_ℓ on the slit domain with about 500 nodes.

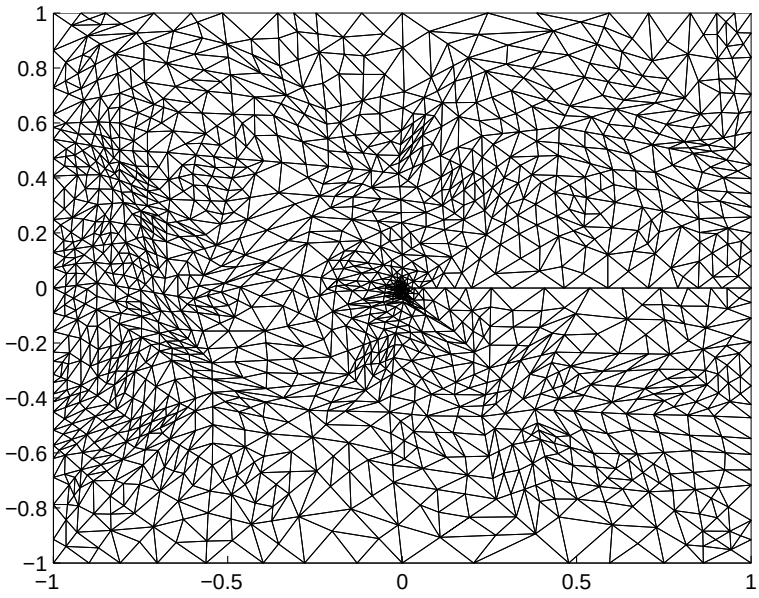

FIGURE 5.27. Perturbed mesh, with 1465 nodes, generated by Algorithm 5.1 with $\beta = (3,0)^T$ for the slit domain.

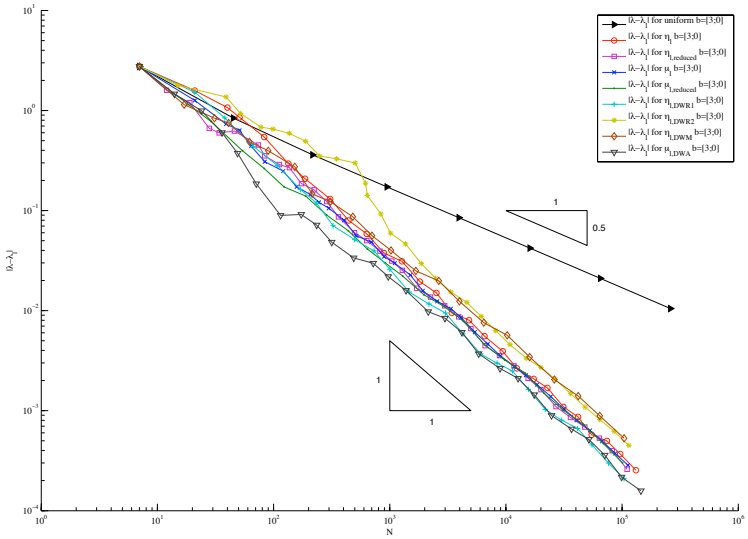

FIGURE 5.28. Eigenvalue errors with $\beta = (3,0)^T$ for a uniform mesh and adaptive meshes generated by η_ℓ, $\eta_{\ell,\text{reduced}}$, μ_ℓ, $\mu_{\ell,\text{reduced}}$, $\eta_{\ell,\text{DWR1}}$, $\eta_{\ell,\text{DWR2}}$, $\eta_{\ell,\text{DWM}}$ and $\mu_{\ell,\text{DWA}}$ on the slit domain.

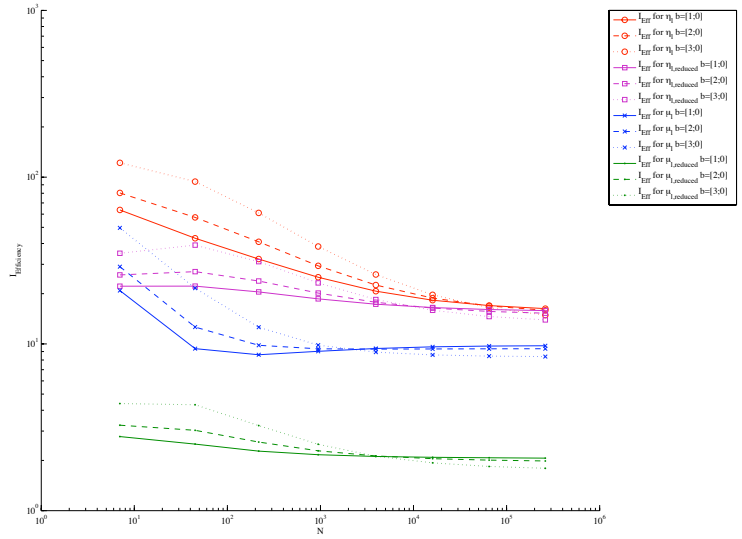

FIGURE 5.29. Efficiency indices for the non-weighted estimators η_ℓ, $\eta_{\ell,\text{reduced}}$, μ_ℓ, $\mu_{\ell,\text{reduced}}$, with convection coefficients $\beta = (1,0)^T$, $\beta = (2,0)^T$ and $\beta = (3,0)^T$ for uniform meshes on the slit domain.

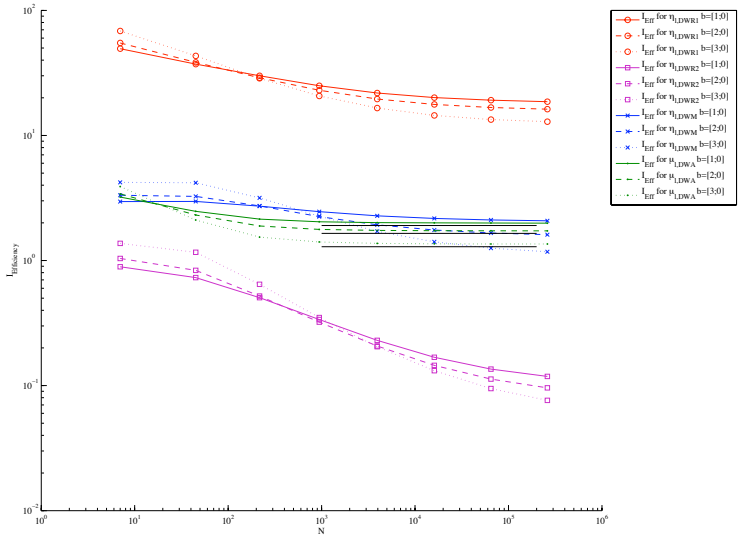

FIGURE 5.30. Efficiency indices for the dual-weighted estimators $\eta_{\ell,\text{DWR1}}$, $\eta_{\ell,\text{DWR2}}$, $\eta_{\ell,\text{DWM}}$ and $\mu_{\ell,\text{DWA}}$ with convection coefficients $\beta = (1,0)^T$, $\beta = (2,0)^T$ and $\beta = (3,0)^T$ for uniform meshes on the slit domain.

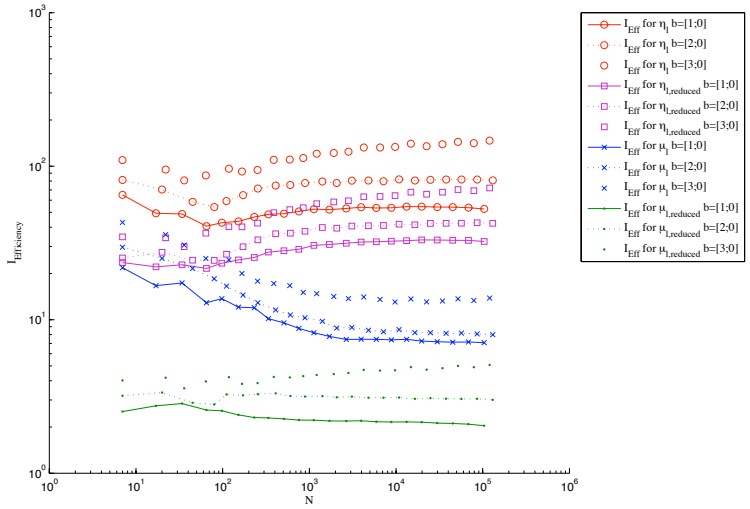

FIGURE 5.31. Efficiency indices for the non-weighted estimators η_ℓ, $\eta_{\ell,\text{reduced}}$, μ_ℓ, $\mu_{\ell,\text{reduced}}$, with convection coefficients $\beta = (1,0)^T$, $\beta = (2,0)^T$ and $\beta = (3,0)^T$ for a sequence of perturbed meshes generated by Algorithm 5.1 on the slit domain.

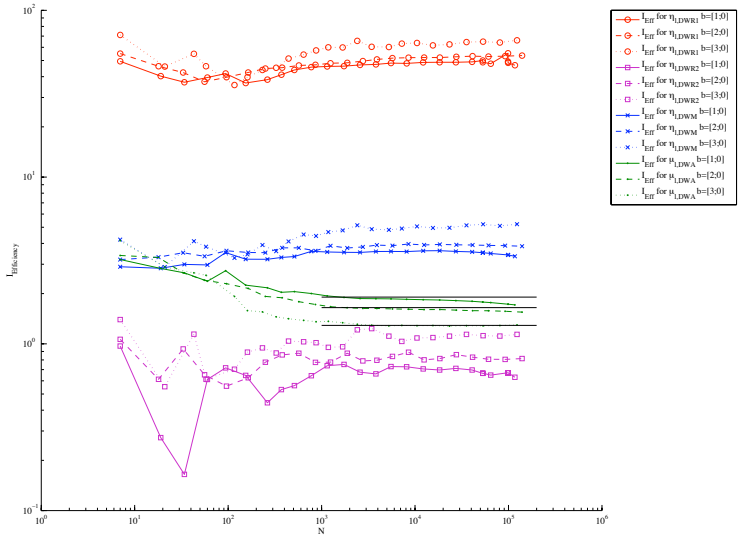

FIGURE 5.32. Efficiency indices for the dual-weighted estimators $\eta_{\ell,\text{DWR1}}$, $\eta_{\ell,\text{DWR2}}$, $\eta_{\ell,\text{DWM}}$ and $\mu_{\ell,\text{DWA}}$ with convection coefficients $\beta = (1,0)^T$, $\beta = (2,0)^T$ and $\beta = (3,0)^T$ for a sequence of perturbed meshes generated by Algorithm 5.1 on the slit domain.

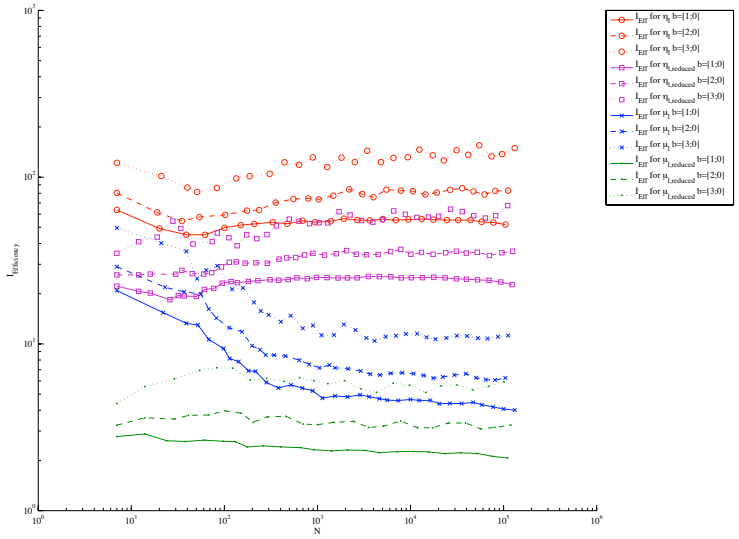

FIGURE 5.33. Efficiency indices for the non-weighted estimators η_ℓ, $\eta_{\ell,\text{reduced}}$, μ_ℓ, $\mu_{\ell,\text{reduced}}$, with convection coefficients $\beta = (1,0)^T$, $\beta = (2,0)^T$ and $\beta = (3,0)^T$ for sequences of meshes generated by the corresponding refinement indicators on the slit domain.

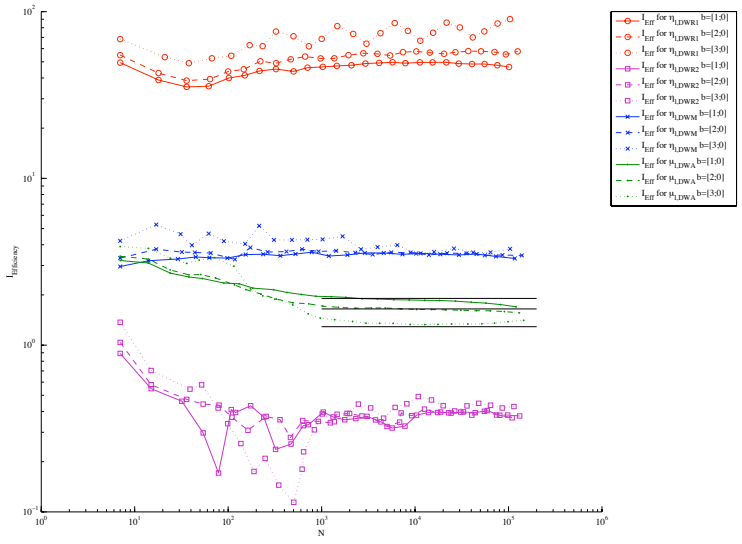

FIGURE 5.34. Efficiency indices for the dual-weighted estimators $\eta_{\ell,\text{DWR1}}$, $\eta_{\ell,\text{DWR2}}$, $\eta_{\ell,\text{DWM}}$ and $\mu_{\ell,\text{DWA}}$ with convection coefficients $\beta = (1,0)^T$, $\beta = (2,0)^T$ and $\beta = (3,0)^T$ for sequences of meshes generated by the corresponding refinement indicators on the slit domain.

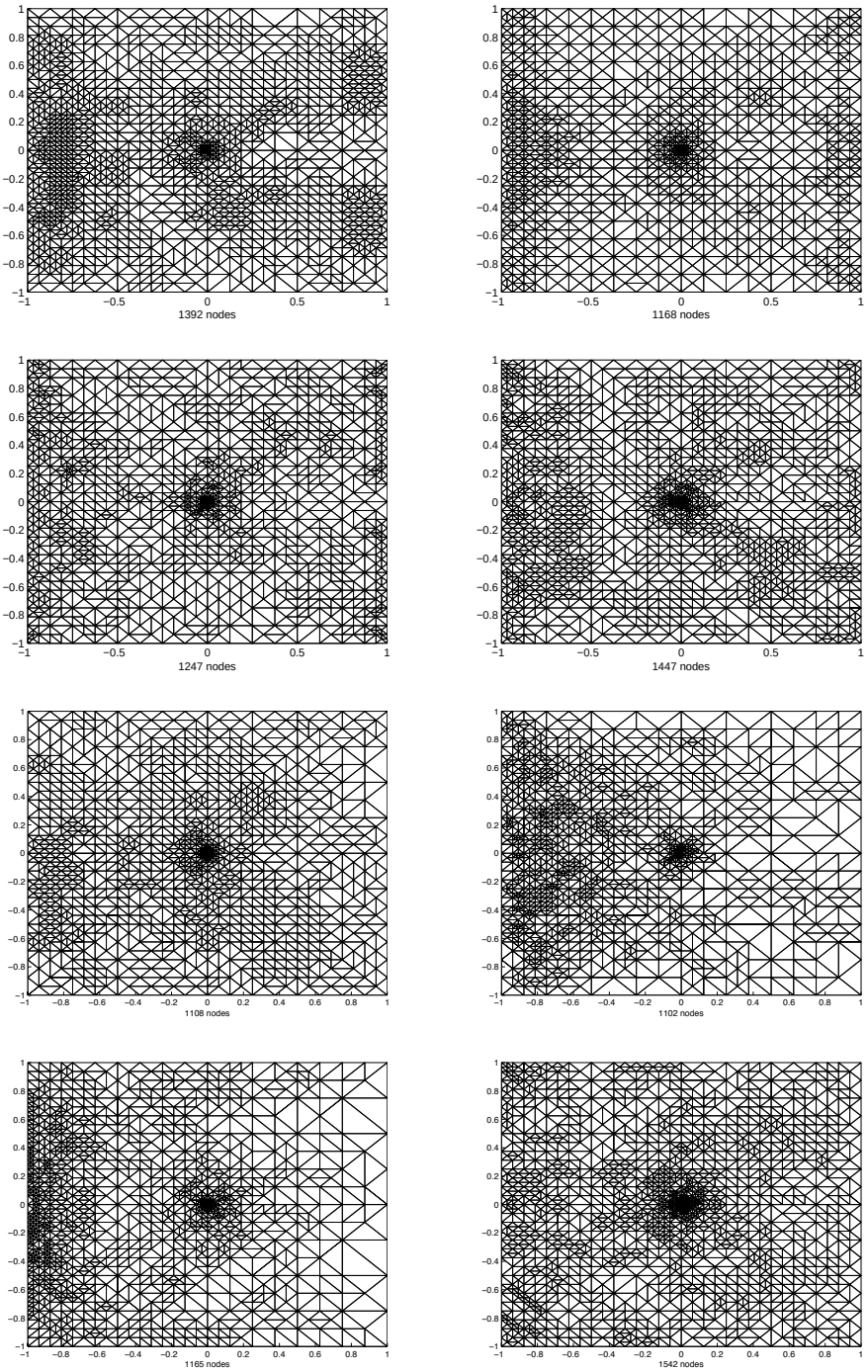

FIGURE 5.35. Meshes with $\beta = (3,0)^T$ generated by the estimators (from left to right and top to bottom) η_ℓ, $\eta_{\ell,\text{reduced}}$, μ_ℓ, $\mu_{\ell,\text{reduced}}$, $\eta_{\ell,\text{DWR1}}$, $\eta_{\ell,\text{DWR2}}$, $\eta_{\ell,\text{DWM}}$ and $\mu_{\ell,\text{DWA}}$ on the slit domain with about 1000 up to 1500 nodes.

German Research Foundation (DFG) under C22 in the Research Center MATHEON. The first author was also supported by the graduate school BMS. The work of the second author was partly supported by the WCU program through KOSEF (R31-2008-000-10049-0).

References

[ACF99] J. Alberty, C. Carstensen, and S.A. Funken, *Remarks around 50 lines of matlab: short finite element implementation*, Numer. Algorithms **20** (1999), 117–137.

[AO00] M. Ainsworth and J.T. Oden, *A posteriori error estimation in finite element analysis*, John Wiley & Sons, Inc., 2000.

[BE03] M. Braack and A. Ern, *A posteriori control of modeling errors and discretization errors*, Multiscale Model. Simul. **1** (2003), no. 2, 221–238.

[BR98] R. Becker and R. Rannacher, *Weighted a posteriori error control in FE methods*, Hans Georg (ed.) et al., ENUMATH 97, 1998.

[BR01] ———, *An optimal control approach to error estimation and mesh adaptation in finite element methods*, Acta Numerica 2000, Cambridge University Press, 2001.

[BR03] W. Bangerth and R. Rannacher, *Adaptive finite element methods for differential equations*, Birkhäuser, Basel, 2003.

[BS02] S.C. Brenner and L.R. Scott, *The mathematical theory of finite element methods*, second ed., Texts in Applied Mathematics, Springer-Verlag, 2002.

[Car03] C. Carstensen, *All first-order averaging techniques for a posteriori finite element error control on unstructured grids are efficient and reliable*, Mathematics of Computation **73** (2003), 1153–1165.

[Car04] ———, *An adaptive mesh-refining algorithm allowing for an H^1 stable L^2 projection onto courant finite element spaces*, Constructive Approximation **20** (2004), 549–564.

[Car05a] ———, *Estimation of higher sobolev norm from lower order approximation*, SIAM J. Numer. Anal. **42** (2005), no. 5, 2136–2147.

[Car05b] ———, *A unifying theory of a posteriori finite element error control*, Numer. Math. **100** (2005), 617–637.

[CB02] C. Carstensen and S. Bartels, *Each averaging technique yields reliable a posteriori error control in FEM on unstructured grids. part i: Lower order conforming, nonconforming and mixed FEM*, Math. Comp. **71** (2002), no. 239, 945 – 969.

[CG08] C. Cartensen and J. Gedicke, *An oscillation-free adaptive FEM for symmetric eigenvalue problems*, Preprint 489, DFG Research Center MATHEON, Straße des 17.Juni 136, D-10623 Berlin, 2008.

[Cha83] F. Chatelin, *Spectral approximation of linear operators*, Academic Press, New York, 1983.

[DPR03] R.G. Durán, C. Padra, and R. Rodrguez, *A posteriori error estimates for the finite element approximation of eigenvalue problems*, Mathematical Models and Methods in Applied Sciences **13** (2003), 1219–1229.

[Eva00] L.C. Evans, *Partial differential equations*, American Mathematical Society, 2000.

[GG09] S. Giani and I.G. Graham, *A convergent adaptive method for elliptic eigenvalue problems*, SIAM J. Numer. Anal. **47** (2009), 1067–1091.

[GMZ08] E.M. Garau, P. Morin, and C. Zuppa, *Convergence of adaptive finite element methods for eigenvalue problems*, Preprint arXiv:0803.0365v1, 2008, http://arxiv.org/abs/0803.0365v1.

[GV96] G.H. Golub and C.F. Van Loan, *Matrix computations*, third ed., 1996.

[HR01] V. Heuveline and R. Rannacher, *A posteriori error control for finite element approximations of elliptic eigenvalue problems*, Advances in Computational Mathematics **15** (2001), 107–138.

[Kat80] T. Kato, *Pertubation theory for linear operators*, Springer, 1980.

[Lar00] M.G. Larson, *A posteriori and a priori error analysis for finite element approximations of self-adjoint elliptic eigenvalue problems*, SIAM J. Numer. Anal. **38** (2000), 608–625.

[MSZ06] D. Mao, L. Shen, and A. Zhou, *Adaptive finite element algorithms for eigenvalue problems based on local averaging type a posteriori error estimates*, Advanced in Computational Mathematics **25** (2006), 135–160.

[OB91] J.E. Osborn and I. Babuška, *Eigenvalue problems*, vol. 2, Handbook of Numerical Analysis, 1991.

[Sau07] S. Sauter, *Finite elements for elliptic eigenvalue problems in the preasymptotic regime*, Preprint 17-2007, Institut für Mathematik der Universität Zürich, Universität Zürich, Winterthurerstrasse 190, CH-8057 Zürich, 2007.

[Ver96] R. Verfürth, *A review of a posteriori error estimation and adaptive mesh-refinement techniques*, Wiley and Teubner, 1996.

[ZZ92] O.C. Zienkiewicz and J.Z. Zhu, *The superconvergent patch recovery and a posteriori error estimates. part 1: The recovery technique*, Int. J. for Numer. Methods in Engineering **33** (1992), 1331 – 1364.

(J. Gedicke) Humboldt-Universität zu Berlin, Unter den Linden 6, 10099 Berlin, Germany

E-mail address: gedicke@mathematik.hu-berlin.de

(C. Carstensen) Humboldt-Universität zu Berlin, Unter den Linden 6, 10099 Berlin, Germany;
Department of Computational Science and Engineering, Yonsei University, 120-749 Seoul, Korea.

E-mail address: cc@mathematik.hu-berlin.de